

# **ELECTROPHYSIOLOGICAL PROPERTIES OF SUBPOPULATIONS OF MELANIN-CONCENTRATING HORMONE NEURONS**

By

© **Rafiat Damilola Adekunle**

A Thesis submitted to the School of Graduate Studies in partial fulfillment of the  
requirements for the degree of

**Master of Science in Medicine (Neuroscience)**

Division of Biomedical Sciences

Faculty of Medicine

Memorial University of Newfoundland

St. John's, Newfoundland and Labrador

May 2024

## ABSTRACT

Melanin-concentrating hormone (MCH) neurons are essential regulators of diverse physiological states including energy homeostasis, sleep-wake cycle, and memory. MCH neurons also occupy different brain regions: the lateral hypothalamic area (LHA), medial hypothalamus (MH) and zona incerta (ZI). Furthermore, a proportion of MCH neurons co-express cocaine and amphetamine regulated transcript (CART). Therefore, we hypothesized that MCH neurons in distinct anatomical areas or with differential CART expression represent functional subgroups to enable them to perform diverse functions. Whole cell patch clamp recording was performed on acute mouse brain slices in three MCH neuron-rich areas: MH, LHA and ZI. Following recording, a subset of cells was immunohistochemically identified as MCH+/CART+ or MCH+/CART- neurons.

MCH neurons in the LHA and MH were more excitable than ZI neurons, firing more action potentials (AP) when stimulated, although no difference was found in the resting membrane potential (RMP) and AP waveform parameters. Additionally, MCH+/CART- neurons had more depolarized RMP and fired more APs than MCH+/CART+ neurons, suggesting that MCH+/CART- neurons are more excitable. Notably, MCH+/CART- neurons displayed an H-current, which was absent in MCH+/CART+ neurons. To our knowledge, this is the first study to describe the presence of H-current in a subpopulation of MCH neurons. These differences in intrinsic membrane properties could contribute to how MCH neuron subpopulations function within the network.

## GENERAL SUMMARY

Melanin-concentrating hormone (MCH) is a peptide produced by a group of neurons in the brain that regulates food intake, sleep, and memory. It has been proposed that there may be subpopulations of these neurons that execute these diverse functions. MCH neurons exist in different parts of the brain like the hypothalamus and zona incerta (ZI). Also, MCH neurons that co-express (or do not co-express) the neuropeptide cocaine and amphetamine regulated transcript (CART) have been described. Through electrophysiological studies, we investigated if MCH neurons in the distinct brain areas and with or without the co-expression of CART show different functional properties. Our results showed that MCH neurons in the lateral hypothalamus are more active than those in the medial hypothalamus and ZI. Most importantly, we newly discovered that MCH+/CART- neurons have a unique property, H-current, that is absent in MCH+/CART+ neurons. Overall, this study discovered subgroups of MCH neurons that may have different functions.

## ACKNOWLEDGEMENTS

I would like to thank my supervisor, Dr. Michiru Hirasawa, for her guidance and mentorship. I would also be forever grateful for her support throughout my masters and medical education. Without your support and continuous encouragement, I don't think I would be where I am today. I would also like to thank my supervisory committee members, Dr. Jacqueline Vanderluit and Dr. Xihua Chen, for their assistance and suggestions. This work would not have been possible without the financial supports from the Faculty of Medicine Research and Graduate Studies, the School of Graduate Studies, the Canadian Institutes of Health Research and Natural Sciences (CIHR) and Engineering Research Council of Canada (NSERC).

Next, I would like to thank past and current members of the Hirasawa lab, Dr. Victoria Linehan, Kanako Kato, Sherri Bowes and Mohammed Sohel Chowdhury for their electrophysiological recordings which I continued to expand on for my thesis. Special thanks to Lisa Fang, Mohammed Sohel Chowdhury and Nick Newhook. Lisa, thank you for teaching me how to patch, the late-night messages and the endless conversations. Sohel, thank you for always supporting me, I truly could not have done this without your help. Nick, thank you for teaching me how to perform immunohistochemistry, and being there to answer all my questions.

Finally, I would like to thank my family and friends. Olufunke and the entire Amadi family, thank you for providing me with a second family, feeding me, and providing continuous support throughout this journey. To my parents, Fatimo and

Monsuru Adekunle, along with my siblings, Adebola, Olamide, Abolore, and Ayomide and my second Mother, Amina Sebbi: thank you! Without you all, this would not have been possible.

## **CO-AUTHORSHIP STATEMENT**

I, Rafiat Damilola Adekunle, designed the experiments with my supervisor Dr. Michiru Hirasawa, for all experimental results in this thesis. In addition to performing a significant portion of the patch clamp recordings, I also performed all data analysis presented within this thesis.

This thesis also includes data collected by current and former members of Dr. Michiru Hirasawa's lab. Specifically, patch clamp recordings were performed by Mohammed Sohel Chowdhury, Dr. Lisa Fang, Sherri Bowes, Kanako Kato, and Dr. Victoria Linehan. Furthermore, immunohistochemistry was performed by Mohammed Sohel Chowdhury, Nick Newhook and Todd Rowe.

## TABLE OF CONTENTS

ABSTRACT .....	II
GENERAL SUMMARY .....	III
ACKNOWLEDGEMENTS .....	IV
CO-AUTHORSHIP STATEMENT .....	VI
LIST OF FIGURES .....	X
LIST OF ABBREVIATIONS .....	XII
CHAPTER 1.....	1
INTRODUCTION.....	1
1.1 HISTORY AND STRUCTURE OF MELANIN-CONCENTRATING HORMONE.....	1
1.2 PHYSIOLOGICAL ROLES OF MCH .....	3
1.2.1 <i>MCH and Energy Homeostasis</i> .....	3
1.2.2 <i>MCH and Glucose Homeostasis</i> .....	4
1.2.3 <i>MCH and Sleep</i> .....	5
1.2.4. <i>MCH and cognition</i> .....	6
1.2.5. <i>MCH and Mood</i> .....	7
1.3 ANATOMICAL SUBPOPULATION OF MCH NEURONS .....	8
1.3.1 <i>Lateral hypothalamus</i> .....	8
1.3.2 <i>Zona Incerta</i> .....	9

1.3.3 <i>Medial Hypothalamus</i> .....	10
1.4 NEUROCHEMICAL SUBPOPULATIONS OF MCH NEURONS .....	11
1.5 SUMMARY AND HYPOTHESIS.....	12
CHAPTER 2.....	14
MATERIALS AND METHODS .....	14
2.1 ANIMAL MODEL.....	14
2.2 SLICE PREPARATION .....	15
2.3 ELECTROPHYSIOLOGICAL RECORDING.....	16
2.4 MCH/CART IMMUNOHISTOCHEMISTRY .....	17
2.5 DATA ANALYSIS.....	18
CHAPTER 3.....	21
RESULTS.....	21
3.1 ANATOMICAL SUBPOPULATIONS OF MCH NEURONS.....	21
3.1.1 <i>Anatomical Distribution of MCH Expression in the Mouse Hypothalamus</i> .....	21
3.1.2 <i>Excitability of Anatomical Subpopulations of MCH Neurons</i> .....	24
3.1.3 <i>Genotype-dependent Differences in Excitability of Anatomical Subpopulations of MCH Neurons</i> .....	29
3.1.4 <i>Excitability of Anatomical Area Subpopulations of MCH Neurons in Male and Female Mice</i> .....	32

3.1.5 Excitability of MCH Neurons from Different Anatomical Areas Held at Subthreshold Potential.....	36
3.2 NEUROCHEMICAL SUBPOPULATIONS OF MCH NEURONS .....	40
3.2.1 Excitability of Neurochemical Subpopulations of MCH Neurons .....	40
.....	43
3.2.2 Excitability of Neurochemical Subpopulations of MCH Neurons in Male and Female Mice .....	45
3.3 ANATOMICAL DISTRIBUTION OF MCH AND CART EXPRESSION IN THE MOUSE HYPOTHALAMUS ..	52
CHAPTER 4.....	57
DISCUSSION.....	57
4.1 ANATOMICAL SUBPOPULATIONS OF MCH NEURONS.....	57
4.2 NEUROCHEMICAL SUBPOPULATIONS OF MCH NEURONS .....	60
4.3 LIMITATIONS OF THE STUDY .....	63
4.4 CONCLUSION .....	64
REFERENCES .....	66
APPENDIX A: ANIMAL CARE ETHICS APPROVAL .....	78

## LIST OF FIGURES

Figure 1: Sample action potential waveform analysis. ....	20
Figure 2: Distribution of MCH neurons in the mouse hypothalamus.....	22
Figure 3: Post hoc immunohistochemical identification of MCH neurons.....	23
Figure 4: Classification of MCH neurons by firing activity. ....	26
Figure 5: Excitability of MCH neurons in distinct anatomical areas. ....	27
Figure 6: Action potential (AP) waveform analysis of anatomical subpopulations of MCH neurons. ....	28
Figure 7: Comparison of MCH neurons from td-tomato and wildtype mice. ....	30
Figure 8 : MCH neurons from td-tomato and wildtype mice. ....	31
Figure 9: Analysis for anatomical differences in MCH neurons from male and female mice.....	34
Figure 10: Analysis of sexual dimorphism in AP properties of MCH neurons. ....	35
Figure 11: MCH neurons from different anatomical areas held at subthreshold potential. ....	<b>Error! Bookmark not defined.</b>
Figure 12: Electrophysiological properties of MCH neurons held at a subthreshold potential.....	39
Figure 13: Post hoc immuno-histochemical confirmation of MCH and CART co-expression. ....	42
Figure 14: MCH neurons display neurochemical differences in excitability. ....	43

Figure 15: Action potential waveform analysis in neurochemical subpopulations of MCH neurons. ....	44
Figure 16: Characteristics of MCH neurons with or without CART co-expression in male mice.....	48
Figure 17: AP waveform analysis of neurochemical subpopulations of MCH from male mice.....	49
Figure 18: Analysis of sexual dimorphism in excitability of CART-expressing MCH neurons .....	50
Figure 19: AP waveform analysis for sex-dependent differences in CART-expressing MCH neurons. ....	51
Figure 20: Immunohistochemistry illustrating the distribution of MCH and CART neurons in the mouse hypothalamus. ....	54
Figure 21: Excitability of MCH+CART+ neurons in distinct hypothalamic areas .....	55
Figure 22: Anatomical area differences among MCH+/CART+ neurons. ....	56

## LIST OF ABBREVIATIONS

3V:	Third Ventricle
ACSF:	Artificial Cerebrospinal Fluid
ANOVA:	Analysis of Variance
AHP:	After Hyperpolarizing Potential
AP:	Action Potential
cAMP:	Cyclic Adenosine Monophosphate
CART:	Cocaine and Amphetamine Regulated Transcript
CNS:	Central Nervous System
CSF:	Cerebrospinal fluid
DMH:	Dorsomedial Hypothalamus
DRN:	Dorsal Raphe Nucleus
GABA:	Gamma-aminobutyric acid
GIRK:	G-protein Gated Inwardly Rectifying Potassium
GPCR:	G-protein Coupled Receptor
HCN Channel:	Hyperpolarization-activated Cyclic Nucleotide Gated Channel
ICV:	Intracerebroventricular
IHy:	Incerto Hypothalamic Area
int:	Internal capsule
kHz:	Kilo Hertz

KO:	Knockout
LHA:	Lateral Hypothalamic Area
MCH:	Melanin-concentrating Hormone
MCHR1:	Melanin-concentrating Hormone Receptor 1
MCx:	Cerebral Motor Cortex
mGluR:	Metabotropic Glutamate Receptor
MH:	Medial Hypothalamus
Min:	Minute
mM:	Millimolar
MRN:	Medial Raphe Nucleus
mRNA:	Messenger Ribonucleic Acid
ms:	Millisecond
mV:	Millivolt
NREM:	Non-Rapid Eye Movement Sleep
OT:	Optic Tract
pA:	Pico-Amps
PBS:	Phosphate Buffered Saline
PPT:	Pedunculo pontine Tegmental Nucleus
NPY:	Neuropeptide Y
REM:	Rapid Eye Movement
Rm:	Membrane Resistance

RMP:	Resting Membrane Potential
SCL-1	Streptococcal collagen-like surface protein-1
SCN:	Suprachiasmatic Nucleus
SEM:	Standard Error of the Mean
VLPO:	Ventrolateral Preoptic Nucleus
WT:	Wildtype
ZI:	Zona Incerta
$\mu\text{m}$ :	Micrometer
$\mu\text{M}$ :	Micromolar

# CHAPTER 1

## INTRODUCTION

### 1.1 History and Structure of Melanin-Concentrating Hormone

Melanin-concentrating hormone (MCH) was first isolated as a 17-amino acid peptide in the chum salmon pituitary (Kawauchi et al., 1983). As its name suggests, MCH was initially only known for its role in pigmentation and skin colour changes in teleost (Kawauchi et al., 1983). Although the first isolation was performed in the pituitary of salmon, it was hypothesized at the time that MCH was likely produced in the hypothalamus. This hypothesis was later confirmed in 1989 when MCH was isolated in the hypothalamus of rats using antiserum raised against salmon MCH (Vaughan et al., 1989). The mammalian MCH is still highly homologous to salmon MCH despite being a cyclic 19-amino acid polypeptide (Vaughan et al., 1989).

The streptococcal collagen-like surface protein-1 (SCL-1), an orphan G-protein coupled receptor (GPCR), was identified almost simultaneously by several groups in 1999 as the natural MCH receptor (Bächner et al., 1999; Chambers et al., 1999; Lembo et al., 1999; Saito et al., 1999), and was later renamed as MCH-receptor 1 (MCHR1). MCHR1 gene expression is widely distributed in the brain. MCHR1 mRNA is prominently expressed throughout the cortex (e.g., orbital, piriform, primary motor cortex, auditory, visual), olfactory region, nucleus accumbens, and striatum (Kokkotou et al., 2001; Saito et al., 2001). MCHR1 mRNA has also been detected in the hippocampus, amygdala,

thalamus, hypothalamus, and brainstem but with notable absence of expression in the cerebellum (Chee et al., 2013; Kokkotou et al., 2001).

The distribution of MCH cells in the brain has been mapped in different species including mice, rats, birds, primates, and humans (Bittencourt et al., 1992; Bittencourt & Elias, 1998; Mouri et al., 1993; Qu et al., 1996; Zamir et al., 1986). In each of these species, MCH-expressing cells are localized in the diencephalon with cell bodies identified extensively in the lateral hypothalamic area (LHA), the zona incerta (ZI), and in the medial hypothalamus including the incerto hypothalamic area (IH<sub>y</sub>), a part of the medial hypothalamus region formerly called the rostromedial zona incerta (Bittencourt et al., 1992; Skofitsch et al., 1985). Outside the diencephalon, MCH mRNA is also expressed in the olfactory tubercle and the pons (Bittencourt et al., 1992).

MCH-expressing neurons project widely throughout the brain in a pattern consistent with MCHR1 expression. These projections include all neocortical areas, thalamus, olfactory tubercle, hippocampal formation, nucleus accumbens, amygdala, hindbrain, and spinal cord (Bittencourt et al., 1992; Bittencourt & Elias, 1998; Haemmerle et al., 2015; Lima et al., 2013; Skofitsch et al., 1985). With the widespread expression of MCHR1 receptors and the broad projections of MCH neurons, it is not surprising that MCH neurons are involved in a wide range of physiological functions including food intake, energy homeostasis, sleep, memory, and mood (Borowsky et al., 2002; Monzon et al., 1999; Qu et al., 1996; Verret et al., 2003).

## 1.2 Physiological Roles of MCH

### 1.2.1 MCH and Energy Homeostasis

The role of MCH in energy balance was first elucidated in 1996 by Qu and colleagues. They proposed that since MCH was prominent in the LHA and ZI; and since these areas are involved in the regulation of feeding behaviours, MCH could be involved in feeding. This proposal was supported when MCH mRNA expression was found to be higher in the hypothalamus of genetically obese *ob/ob* mice (Qu et al., 1996). An increase in MCH mRNA was also observed after fasting in both normal and obese mice (Presse et al., 1996; Qu et al., 1996). In addition, chronic intracerebroventricular (ICV) injection of MCH into the lateral ventricles of rats increased their food consumption and body weight gain (Abbott et al., 2003; Gomori et al., 2003; Qu et al., 1996). Furthermore, mice with MCH overexpression had increased intake of high fat diet and weight gain than wildtype (WT) animals (Ludwig et al., 2001). Chemogenetic activation of MCH neurons that project to the third ventricle and release MCH into the cerebrospinal fluid (CSF) increased feeding (Noble et al., 2018), suggesting this may be a signalling pathway for MCH's role in food intake.

Further confirmation of MCH role in energy balance was performed with genetic animal model studies. It has been shown that rodents lacking MCH (Shimada et al., 1998) or MCH1R (Chen et al., 2002; Marsh et al., 2002) are lean, hypophagic and have increased energy expenditure. In fact, mice with MCH ablated (MCH-KO mice) had less weight gain compared to their WT counterparts. This result is mainly because they had

increased energy expenditure (Kokkotou et al., 2005; Segal-Lieberman et al., 2003).

Interestingly, MCH-KO mice had increased basal physical activity that further increased when the animals were placed on high fat diet (Kokkotou et al., 2005).

Collectively, these show that not only does MCH increase food intake, but also reduces energy expenditure leading to weight gain. This is supported by chronic ICV infusion of MCH, which results in increased food intake, body weight, and fat mass with decreased body temperature and energy expenditure (Glick et al., 2009).

### **1.2.2 MCH and Glucose Homeostasis**

MCH neurons have also been shown to be involved with glucose homeostasis. MCH neurons are excited by physiological levels of glucose (between 0.2 mM and 5 mM), displaying higher action potential frequency when glucose concentration is increased (Burdakov et al., 2005; Kosse et al., 2015). MCH ablated aged mice were more insulin sensitive and displayed better glucose tolerance than control mice (Jeon et al., 2006). Interestingly, a reduction in locomotor activity due to age was diminished in transgenic mice lacking MCH compared to wildtype littermates (Jeon et al., 2006). High levels of insulin have also been shown to increase the excitability of MCH neurons (Hausen et al., 2016; Verret et al., 2003). Food intake causes a spike in blood glucose and release of insulin; this spike in glucose and insulin then activates MCH neurons promoting sleep and energy conservation. However, when glucose level falls, the

reduced excitability of MCH neurons may suppress sleep and induce locomotor activity for food seeking.

### **1.2.3 MCH and Sleep**

MCH neurons are also well recognized for their role in the sleep-wake cycle. Early works on the role of MCH in sleep showed that there was increased neural activity of MCH neurons during rapid eye movement (REM) sleep hypersomnia (Verret et al., 2003). In fact, ICV injection of MCH led to an increase in REM and non-REM sleep quantities, with higher increase in REM sleep (Hassani et al., 2009; Verret et al., 2003). Conversely, MCHR1 antagonist injection in rats decreased REM and non-REM sleep bouts (Ahnaou et al., 2008). Consistently, mice with their MCH knocked out showed a reduction in non-REM sleep and an increase in wake period (Adamantidis et al., 2008). Furthermore, optogenetic activation of MCH neurons prolongs REM and non-REM sleep and stimulates the transition into REM sleep (Blanco-Centurion et al., 2016; Jégo et al., 2013; Vetrivelan et al., 2016). Moreover, optogenetic activation during the wake cycle greatly increased total sleep duration (Konadhode et al., 2013), (Konadhode et al., 2014). Taken together, these findings indicate that MCH increases sleep at the expense of wake time.

#### **1.2.4. MCH and cognition**

MCH is also believed to play a role in learning and memory. One of the early works showed that infusion of MCH peptide into the hippocampus of rats improved memory during a step-down inhibitory avoidance test (Monzon et al., 1999). The step-down inhibitory avoidance test is a common memory test where animals are placed on a platform and the time to step down from the platform (latency) is measured. During training, the animals are given an electrical shock once they step down fully from the platform onto the grid. The latency to step down is then measured during the test, as animals that take longer to step down are said to have better memory about the foot shock than those that step down too quickly. In the Monzon and colleagues experiments, the increase in latency lasted up to four hours after MCH injection (experiment repeated four hours after injection). Consistent with the work of Monzon and colleagues, perfusion of rat hippocampal slices with MCH led to an increase in hippocampal long-term synaptic potentiation (Varas et al., 2002). Furthermore, disruption of MCHR1 in mice has confirmed the importance of MCH in memory. Adamantidis and colleague found that MCHR1 KO mice showed impaired memory retention when tested in the one-trial inhibitory avoidance test, a similar paradigm to the step-down inhibitory avoidance test (Adamantidis & de Lecea, 2009). MCH-R1 KO mice showed a reduction in step down latency compared to WT animals at both one- and six-days post-training. Consistent with these findings, mice with their MCH neurons ablated also performed poorly on short term memory tasks compared to WT mice (Le

Barillier et al., 2015). Together, these studies provide evidence that the loss of MCH neurons or MCH receptors impairs learning and memory retention.

### **1.2.5. MCH and Mood and Anxiety**

MCH is also believed to be involved in anxiety and depression. Previous research has shown that MCH1R antagonists acted like anxiolytics in animal models of anxiety (Borowsky et al., 2002). Also, local application of MCHR1 antagonist into the nucleus accumbens shell (Georgescu et al., 2005) or acute and chronic oral dosing of an MCHR1 antagonist (David et al., 2007) resulted in an anti-depressant effect (David et al., 2007). Moreover, genetically knocking out MCHR1 caused anxiolytic-like effects in animal models of anxiety (Smith et al., 2006). Conversely, ICV injection of MCH in mice produced anxiety-like behaviour assessed by an elevated plus maze, a widely used experimental paradigm for testing anxiety (Smith et al., 2006).

In addition, microinjections of MCH into the dorsal raphe nucleus (DRN, Lagos et al., 2011) or the median raphe nucleus (MRN, López Hill et al., 2013) evoked a depressive-like behaviour in mice during the forced swim test, a common paradigm for testing anti-depressant activity. This effect on depression-related behaviour could be mediated through their connections with serotonergic neurons that are present in the DRN and MRN, known for their role in the pathophysiology of major depressive disorder (Adell et al., 2002; Bittencourt et al., 1992; Saito et al., 2001; Torterolo et al., 2008).

Taken together, these reports show that MCH may induce anxiety and depression-related behaviours.

### **1.3 Anatomical Subpopulation of MCH Neurons**

With the range of physiological functions in which MCH neurons are involved, it has been proposed that different subpopulations of MCH neurons may be present in the brain that perform these various functions. Indeed, research has shown that MCH neurons may be segregated anatomically, as they occupy distinct parts of the hypothalamus, and may also be neurochemically heterogeneous (Bittencourt et al., 1992; Cvetkovic et al., 2004).

MCH-containing neurons are localized exclusively in the diencephalon, including different parts of the hypothalamus and ZI (Bittencourt et al., 1992). Antisera raised against rat MCH was first used to determine the anatomical areas of the brain that MCH-expressing cells occupy (Bittencourt et al., 1992). From this staining, MCH neurons were prominently found in the LHA and ZI; and found scattered in the medial zone of the hypothalamus.

#### **1.3.1 Lateral hypothalamus**

Several studies have shown that MCH neurons in distinct areas may have different projection targets. One such study, (Elias et al., 2008) showed that unique LHA MCH neurons project to either the cerebral motor cortex (MCx) or pedunclopontine

tegmental nucleus (PPT) and only a select few projected to both. The authors injected separately or simultaneously True Blue and Diamidino Yellow into the MCx and PPT, and they observed retrogradely labelled MCH neurons most abundantly in the LHA. The MCx area the authors picked was thought to be related to motor control and having the highest concentration of MCH terminals. These LHA MCH neurons projecting to the MCx may be responsible for mediating the sedentary effects of MCH by reducing locomotor activity and energy expenditure. Also, the PPT is implicated in the control of wake-sleep cycle, as neurons in the PPT fire at increased rate during REM sleep (Steriade et al., 1990). It is likely that MCH innervation of the PPT provides an anatomical basis by which MCH increases REM sleep.

### **1.3.2 Zona Incerta**

The zona incerta is another notable area of the diencephalon where MCH is located. The main functions of the “zone of uncertainty” as it is literally called has not been fully elucidated. However, there have been some proposals as to its function in locomotion, arousal, attention, anxiety, and motivation (Wang et al., 2020). MCH neurons are found mainly in the medial ZI and project widely throughout the brain ranging from the cerebral cortex, the medial septal nucleus and other hypothalamic areas, and to the spinal cord (Bittencourt & Elias, 1998; Mitrofanis, 2005; Sita et al., 2003; Wang et al., 2020). Because of its extensive projections throughout the central nervous system (CNS), the ZI has been thought to be an integrative center. Recently, a

study showed that GABAergic neurons in the ZI promoted sleep, likely through their projections to the LHA (Liu et al., 2017). Another study showed that some ZI neurons were excited during starvation, which led to increased food intake (Zhang & van den Pol, 2017). In summary, the ZI is a diverse area of the brain, and MCH neurons in this area may need to be studied as a separate population.

### **1.3.3 Medial Hypothalamus**

MCH neurons are spread widely in the hypothalamus including the dorsomedial hypothalamus (DMH). The DMH is a crucial brain area that is involved in the regulation of wide variety of physiological and behavioral circadian rhythms (Chou et al., 2003; Faber et al., 2021; Gooley et al., 2006; L. Li et al., 2022). The DMH is considered appetite-stimulating as lesions of DMH resulted in reduced food intake (Bellinger & Bernardis, 2002). Activation of cholinergic neurons within the DMH promotes food intake and overnight fasting increases the activity of DMH cholinergic neurons implying that these neurons sense reduced nutrient availability and increase their activity to promote food intake (Groessl et al., 2013; Jeong et al., 2017). The DMH has also been implicated in the regulation of the sleep-wake cycle. Lesions of the DMH resulted in increased REM and NREM sleep while daily wakefulness time was markedly reduced (Chou et al., 2003; L. Li et al., 2022). Furthermore, DMH area lesions reduced overall daily locomotor activity (Chou et al., 2003). Expectedly, the DMH receives inputs from the suprachiasmatic nucleus (SCN, a brain region that regulates circadian rhythm) and sends projections to brain areas

critical for sleep-wake control, feeding and locomotion (Dimicco & Zaretsky, 2007; Faber et al., 2021; Gooley et al., 2006; Groessl et al., 2013). These projections include GABAergic neurons to the ventrolateral preoptic nucleus (VLPO, area involved in sleep control) and glutamatergic neurons to the LHA (an area known for its orexigenic effect; Chou et al., 2003; Lu et al., 2000; Sherin et al., 1996).

#### **1.4 Neurochemical Subpopulations of MCH Neurons**

Cocaine and amphetamine regulated transcript (CART) is a neuropeptide that was first characterized after it was found to be upregulated in the brain of rodents acutely injected with cocaine or amphetamine (Douglass et al., 1995). Several later studies demonstrated that the CART transcript was constitutively expressed in the brain, with CART being the third most abundantly expressed mRNA in the hypothalamus (Gautvik et al., 1996; Koylu et al., 1997; Smith et al., 1997). The widespread expression of CART in the hypothalamus raises a hypothesis that it might play a role in energy homeostasis. In support of this, several studies have shown CART action in regulating feeding behaviour. For instance, ICV injection of CART peptide inhibits feeding while the administration of CART anti-serum increases food intake (Aja et al., 2001; Lambert et al., 1998; Rogge et al., 2008). CART, like MCH, has also been connected to memory function. For example, the treatment of Alzheimer's model mice with CART peptide ameliorated memory deficits, with improvement in synaptic ultrastructure and long-term potentiation in the hippocampus (Yin et al., 2017).

A previous study showed the expression of CART in approximately 66% of MCH neurons in the rat hypothalamus (Cvetkovic et al., 2004). The MCH-positive CART-positive (MCH+/CART+) neurons were found predominantly in the LHA and ZI, while MCH+/CART- neurons were observed in the LHA and the perifornical region. In MCH-rich areas, single labelled CART-positive neurons (MCH-/CART+) neurons are rare, although they have been observed in the arcuate nucleus. Interestingly in rats, retrograde tracing shows that MCH+/CART+ neurons and MCH+/CART- neurons project to different parts of the brain. MCH+/CART- neurons preferentially project towards the spinal cord, while MCH+/CART+ neurons send ascending projections to innervate the cerebral cortex and medial septal complex (Cvetkovic et al., 2004). However, species differences have been noted. While a similar proportion of MCH neurons co-express CART in mice (60%), only about 60% of MCH+/CART+ neurons projected to the cortex in mice compared to 80% in rats (Croizier et al., 2010; Cvetkovic et al., 2004). Despite the species difference, the presence of CART in some, but not all, MCH neurons supports the notion that there are distinct neurochemical subpopulations of MCH neurons that mediate diverse functions.

### **1.5 Summary and Hypothesis**

It is apparent that MCH neurons play extensive roles in many physiological functions including food intake, sleep homeostasis and cognitive functions. Available evidence suggests that there are subpopulations of MCH neurons that can be distinguished by their anatomical localizations or neurochemical phenotype. Despite

this, past studies investigating the electrophysiological properties of MCH neurons at the cellular level have treated these cells as a single population. As a result, the specific subpopulations of MCH neurons that may undertake certain physiological functions like sleep, energy homeostasis, cannot be differentiated. Therefore, we hypothesized that subpopulations of MCH neurons exist that are electrophysiologically different. Using whole cell patch clamp technique in combination with immunohistochemistry, I examined anatomical and neurochemical subpopulations of MCH neurons to determine differences in their electrophysiological properties. Such differences may be important for shaping specific patterns of activity needed to produce certain functional outcomes (e.g., food intake, sleep, or memory consolidation).

## CHAPTER 2

### MATERIALS AND METHODS

#### 2.1 Animal Model

All animal experiments followed the guidelines of the Canadian Council on Animal Care and were approved by Memorial University Institutional Animal Care Committee.

C57BL/6NCrl mice were obtained from Charles River Laboratory, while MCH-tdTomato mice were bred at Memorial University and used to visualize MCH-expressing neurons. MCH-tdTomato mice were generated by crossing a *Mch-cre* mouse (originally generated by Dr. Bradford Lowell, Harvard University and breeders were kindly provided by Dr. Melissa Chee, Carleton University (Kong et al., 2010); have been crossed with C57BL/6 mice for many generations) with a cre-dependent tdTomato reporter mouse congenic on the C57BL/6J genetic background (stock number 007909, Jackson Laboratory) (Madisen et al., 2010). *Mch-cre* mice selectively express cre-recombinase under the MCH promoter. The tdTomato reporter mouse on the other hand has a lox-P flanked STOP cassette that prevents the fluorescent protein tdTomato from being transcribed in the absence of cre recombinase. In essence, when *Mch-cre* mouse is bred with cre-dependent tdTomato reporter mouse, cre recombinase excises the STOP sequence selectively in MCH neurons so tdTomato is only expressed by MCH neurons in the offspring.

Previous research from our lab has shown that excitability of MCH neurons reach maturity level by 7 weeks in rats and remain stable (Linehan & Hirasawa, 2018). As mice used in the present experiments were 6-12 weeks old, MCH neurons included in the analysis were considered mature. Animals were kept on a 12/12 h light/dark cycle and fed *ad libitum* with standard chow (Prolab RMH 3000).

## 2.2 Slice Preparation

Mice were deeply anesthetized with isoflurane and decapitated. Coronal slices (250  $\mu\text{m}$ ) of the hypothalamus were obtained with the vibratome (VT-1000, Leica Microsystems) in cold artificial cerebrospinal fluid (ACSF) containing (mM): 126 NaCl, 2.5 KCl, 2 CaCl<sub>2</sub>, 1.2 NaH<sub>2</sub>PO<sub>4</sub>, 1.2 MgCl<sub>2</sub>, 18 NaHCO<sub>3</sub>, 2.5 glucose, and bubbled with 95% O<sub>2</sub>/ 5% CO<sub>2</sub>. Slices were then incubated in ACSF for 30 min at 32°C. Alternatively, slices were incubated in recovery solution (in mM: 92 NMDG, 2.5 KCl, 1.25 NaH<sub>2</sub>PO<sub>4</sub>, 30 NaHCO<sub>3</sub>, 20 HEPES, 25 glucose, 5 ascorbic acid, 2 thiourea, 3 sodium pyruvate, 10 MgSO<sub>4</sub>.7H<sub>2</sub>O, and 0.5 CaCl<sub>2</sub>.2H<sub>2</sub>O) for 15 min before being transferred into ACSF for another 15 min for a total of 30 min at 32°C. Following the recovery period, slices were left in ACSF at room temperature until recording. All solutions were continuously bubbled with 95% O<sub>2</sub>/ 5% CO<sub>2</sub>. No recovery solution-dependent differences in electrophysiological parameters were found in identified MCH neurons (data not shown), thus data from slices incubated in regular ACSF or recovery solution was combined.

### 2.3 Electrophysiological Recording

Hemisected brain slices were placed in the recording chamber and perfused continuously with ACSF. Whole cell patch clamping was performed using a Multiclamp 700B and pClamp 10 software (Molecular Devices). An internal solution (composed of, in mM: 123 K-gluconate, 2 MgCl<sub>2</sub>, 1 KCl, 0.2 EGTA, 10 HEPES, 5 Na<sub>2</sub>ATP, 0.3 NaGTP, and 2.7 biocytin) was used to fill glass electrodes with a tip resistance of 3-5 MΩ). An infrared differential interference contrast microscope (DM LFS A, Leica Microsystems) was used to visualize neurons. Once whole-cell configuration was attained, a series of test pulses was applied in voltage clamp with the holding potential of -70 mV to monitor membrane resistance. Series/access resistance and whole cell capacitance were also monitored and cells with series/access resistance greater than 25 MΩ were not used for analysis. All electrophysiological recordings were filtered at 5kHz and acquired at 10kHz. Once whole cell mode was attained, a series of hyperpolarizing and depolarizing current (600 ms) in 50 pA increments were applied in current clamp mode to record passive and active membrane properties.

Whole-cell patch clamp recordings were made from red immunofluorescent neurons (in td-Tomato mice) and select neurons in C57BL/NCrl or cre-negative littermates from tdTomato breeding colony. MCH neurons were scattered in clusters within three anatomical areas and were classified accordingly: the ZI, LHA (lateral to the fornix) and medial hypothalamus (MH, medial to the fornix) according to the annotation in the Allen Mouse Brain Reference Atlas (<https://mouse.brain-map.org/static/atlas>).

## 2.4 MCH/CART Immunohistochemistry

Following the recording, patched cells from wildtype mice were further confirmed as MCH immunopositive using immunohistochemistry. A subset of recorded cells was also stained for CART peptide. For immunohistochemical staining of recorded cells from MCH-tdTomato mice, brain slices were fixed individually in 10% formalin overnight at 4°C following electrophysiology, then washed three times in PBS before the addition of primary antibodies in 96-well plate. For CART detection, Slices were incubated in rabbit anti-CART polyclonal IgG (1:500, Phoenix Pharmaceuticals/H-003-62) for 3 days at 4°C. Slices were then washed with PBS and treated for 3 hours at room temperature with Alexa 488-conjugated anti-rabbit antibody (1:500, Invitrogen/A21206) and AMCA-streptavidin to visualize biocytin (1:500 dilution, Jackson ImmunoResearch/016-150-084).

C57BL/NCrl or cre-negative-tdTomato mice brain slices were also fixed in 10% formalin overnight at 4°C then washed three times in PBS before the addition of primary antibodies. Slices were incubated in goat anti-MCH antibody (1:500, Santa Cruz Biotechnology Inc./SC14509) with or without rabbit anti-CART polyclonal IgG (1:500, Phoenix Pharmaceuticals/H-003-62). Slices were then washed with PBS and treated for 3 hours at room temperature with appropriate combination of secondary antibodies and AMCA-streptavidin.

## 2.5 Data Analysis

For patched neurons that were immuno-confirmed to be MCH neurons or expressed tdTomato, resting membrane potential (RMP), number of action potential (AP), and latency to first spike were assessed using Clampfit10 (Molecular Devices). RMP was measured when no current was injected, and the cell was not firing. Active membrane properties were assessed using recordings during the application of a series of current injections, where 600-ms positive and negative currents with varying amplitude were applied through the recording pipette. Specifically, **number of AP** was the number of spikes during 600-ms positive driving current injections; **latency to first spike** was the time from the onset of these current injection to the first AP. AP waveform was also analysed using the previously documented methods (Linehan & Hirasawa, 2018): **AP threshold** was the membrane potential where the slope of the trace was 10 mV/ms; **AP amplitude** was the membrane potential from the baseline to the peak, where baseline is defined as the membrane potential 30 ms before the threshold; **AP peak** was the membrane potential at the tip of the AP; **half-width** was the duration of the AP at half AP amplitude; and **afterhyperpolarization (AHP) amplitude** was membrane potential from baseline to the peak of AHP (Figure 1A). In some MCH neurons, even the largest current injection (+200 pA) elicited no AP, so the duration of current injection (600 ms) was assigned as the first spike latency and AP waveform analysis was not performed. In addition, some MCH neurons fired AP immediately after the start of current injection, so the second AP (instead of the first) was used for AP waveform analysis in these cells. **H-**

**current amplitude** was the difference between the peak of membrane hyperpolarization and the steady state potential during hyperpolarizing (-200 pA) current injection (Figure 1B). All membrane potentials were corrected for the liquid junction potential, which was -14.9 mV.

Statistical tests were performed using Prism 9 (GraphPad Software Inc., San Diego, CA, USA), including unpaired t-test, one-way and two-way analysis of variance (ANOVA) and chi-square test as appropriate. When significance was found with ANOVA, *post hoc* Sidak's multiple comparison tests were performed, as indicated appropriate by Prism 9. Normality distribution was tested and for comparisons where variance was not equal, non-parametric tests (Mann-Whitney and Kruskal-Wallis for 2 and 3 groups comparison, respectively) were performed. The main effects of ANOVA are indicated in the Results while the post-test results are shown in the figures. Results are presented as mean  $\pm$  SEM.  $P < 0.05$  was considered statistically significant. Number of cells and animals used for each experiment are described as: n/N where "n" represents the number of MCH neurons and "N" the number of mice.

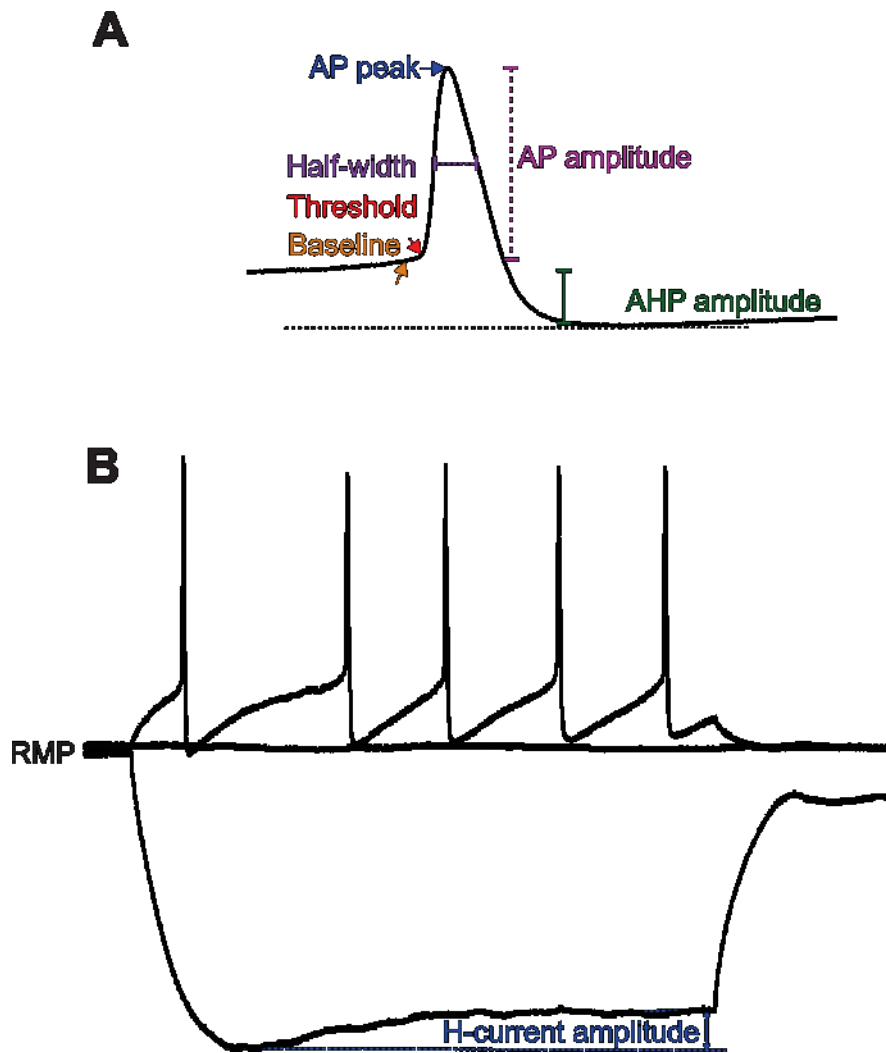


**Figure 1: Sample action potential waveform analysis.**

- (A) Sample image of an action potential (AP) waveform analysis showing resting membrane potential (RMP), threshold, AP peak, AP amplitude, and afterhyperpolarization (AHP) amplitude.
- (B) Sample image of a current clamp recording of an active MCH neuron indicating the H-current amplitude.

## CHAPTER 3

### RESULTS

#### 3.1 Anatomical Subpopulations of MCH Neurons

##### 3.1.1 Anatomical Distribution of MCH Expression in the Mouse Hypothalamus

The specific distribution of MCH neurons was characterized using immunohistochemistry. MCH neurons were distributed extensively in the hypothalamus as shown in Figure 2, and appeared in clusters, including the LHA (defined as the area located ventral to the ZI, lateral to the fornix and medial to the subthalamic nucleus), MH (defined as the area medial to the fornix and mammillothalamic tract, and lateral to the third ventricle), and ZI, with most distribution in the LHA. This distribution was consistent in MCH-tdTomato and wildtype mice (Figure 2). Consequently, patch clamping experiments on MCH neurons selected from these three areas were analyzed and compared to determine if there were any anatomical differences in electrophysiological properties. Ninety-six out of 99 biocytin-filled cells were confirmed as MCH neurons using immunohistochemistry, equivalent to a 97% success rate (Figure 3); 3 cells were MCH immunonegative. Following confirmation of the neurochemical phenotype of the patched cells, the electrophysiological properties of confirmed MCH neurons were analyzed.

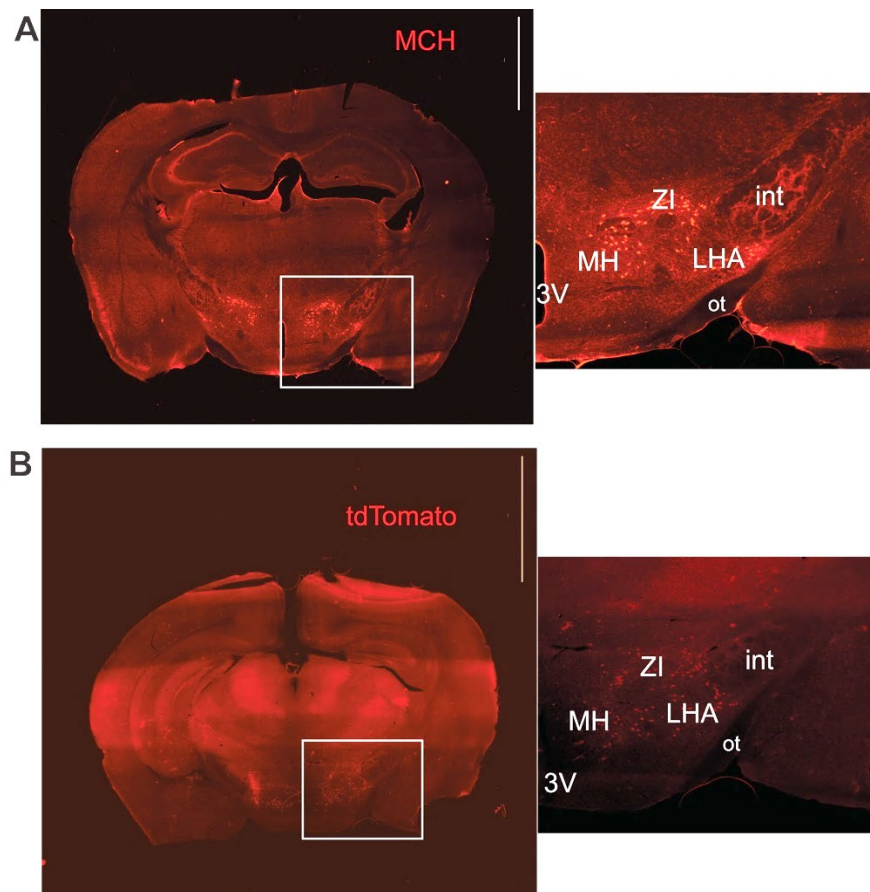


**Figure 2: Distribution of MCH neurons in the mouse hypothalamus.**

- (A) Distribution of MCH neurons on coronal sections through the hypothalamus of a wildtype C57BL mouse visualized by immunohistochemistry against MCH peptide.
- (B) Distribution of MCH neurons on coronal slices of the hypothalamus of an MCH-td tomato mouse.

Scale bar: 500  $\mu$ m; 3V: third ventricle, int: internal capsule, ot: optic tract, LHA: lateral hypothalamic area, MH: medial hypothalamus, ZI: zona incerta

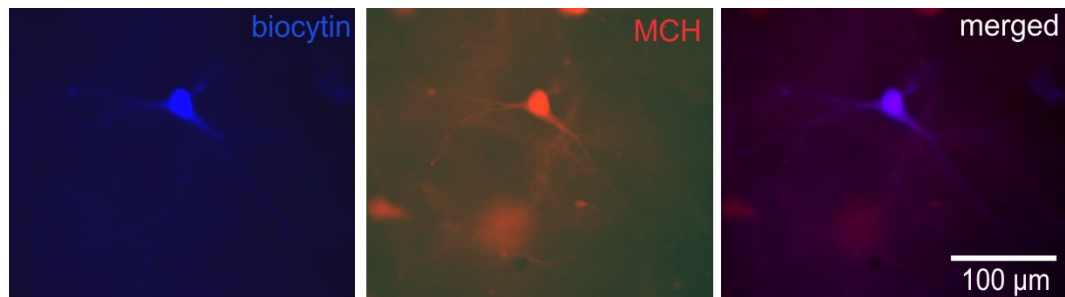


**Figure 3: Post hoc immunohistochemical identification of MCH neurons.**

Sample image of a confirmed MCH neuron. Post hoc staining of biocytin filled cell (blue; left) showing co-localization with MCH peptide (red; middle), confirmed by the merged image (right).

### 3.1.2 Excitability of Anatomical Subpopulations of MCH Neurons

MCH neurons from the ZI, LHA and MH were treated as different subgroups and their intrinsic excitability was examined and compared. Notably, even with maximum current injections (+200 pA), some of the cells did not fire any action potentials (Figure 4 A, B). Analysis of the proportion of cells that fired or did not fire action potential in the three areas showed statistical difference (Chi-square test;  $p = 0.0192$ , Figure 4B).

There were no differences in membrane resistance noted among the three anatomical subgroups (ZI  $n/N = 39/26$ , LHA  $n/N = 20/12$ , MH  $n/N = 42/26$ ;  $p = 0.8731$ , one-way ANOVA; Figure 5B) or the RMP ( $p = 0.4304$ , one-way ANOVA; Figure 5A, C). However, there were significant differences observed in number of AP and first spike latency among the three areas with positive current injection. A two-way ANOVA was performed to analyze the effect of anatomical area and positive current injection on MCH neuron excitability. There was a statistically significant main effect for positive current injection and anatomical area on the number of AP (current injection:  $p < 0.0001$ ; anatomical area:  $p < 0.0001$ , interaction:  $p=0.1542$ ) and latency to first spike (current injection:  $p = 0.0023$ ; anatomical area:  $p < 0.0001$ , interaction:  $p = 0.7522$ ). Post-hoc Tukey's multiple comparisons test showed that MCH neurons from the ZI responded with lower number of AP (Figure 5A, D) and longer latency to first spike compared to MCH neurons in the LHA and MH ( $p < 0.0001$ , one-way ANOVA; Figure 5E).

Furthermore, analysis of AP waveform revealed that there were no differences in threshold (ZI  $n/N = 9/9$ , LHA  $n/N = 9/7$ , MH  $n/N = 25/17$ ;  $p = 0.8168$ , one-way ANOVA;

Figure 6B) among the areas. However, there was difference in AP peak ( $p = 0.0281$ , one-way ANOVA; Figure 6C), AP amplitude ( $p = 0.0459$ , one-way ANOVA; Figure 6D) and half-width ( $p = 0.0039$ , one-way ANOVA; Figure 6E) where AP peak and AP amplitude were higher in LHA than ZI MCH cells, and half-width was shorter in LHA cells than ZI and MH cells. There were no differences in AHP amplitude ( $p = 0.1630$ , one-way ANOVA; Figure 6F). Overall, these results suggest that LHA MCH neurons are more excitable than ZI and MH MCH neurons.

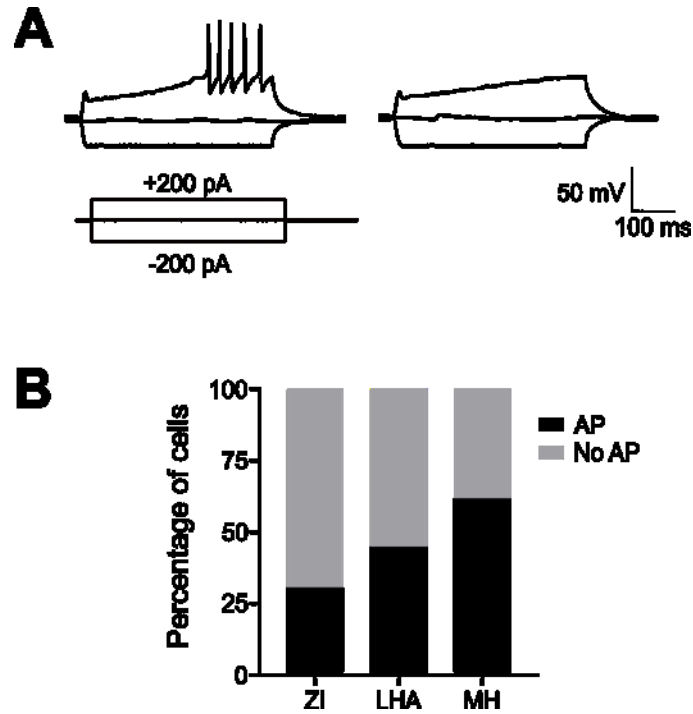


**Figure 4: Classification of MCH neurons by firing activity.**

(A) Sample current clamp recording from an active MCH neuron firing five action potentials (APs, left) and sample of a silent MCH neuron (no AP) with 200-pA current injection.

(B) Proportion of MCH cells in the three areas that did or did not fire an action potential with positive current injections. Analysis with Chi-square test.

ZI: zona incerta, LHA: lateral hypothalamus, MH: medial hypothalamus

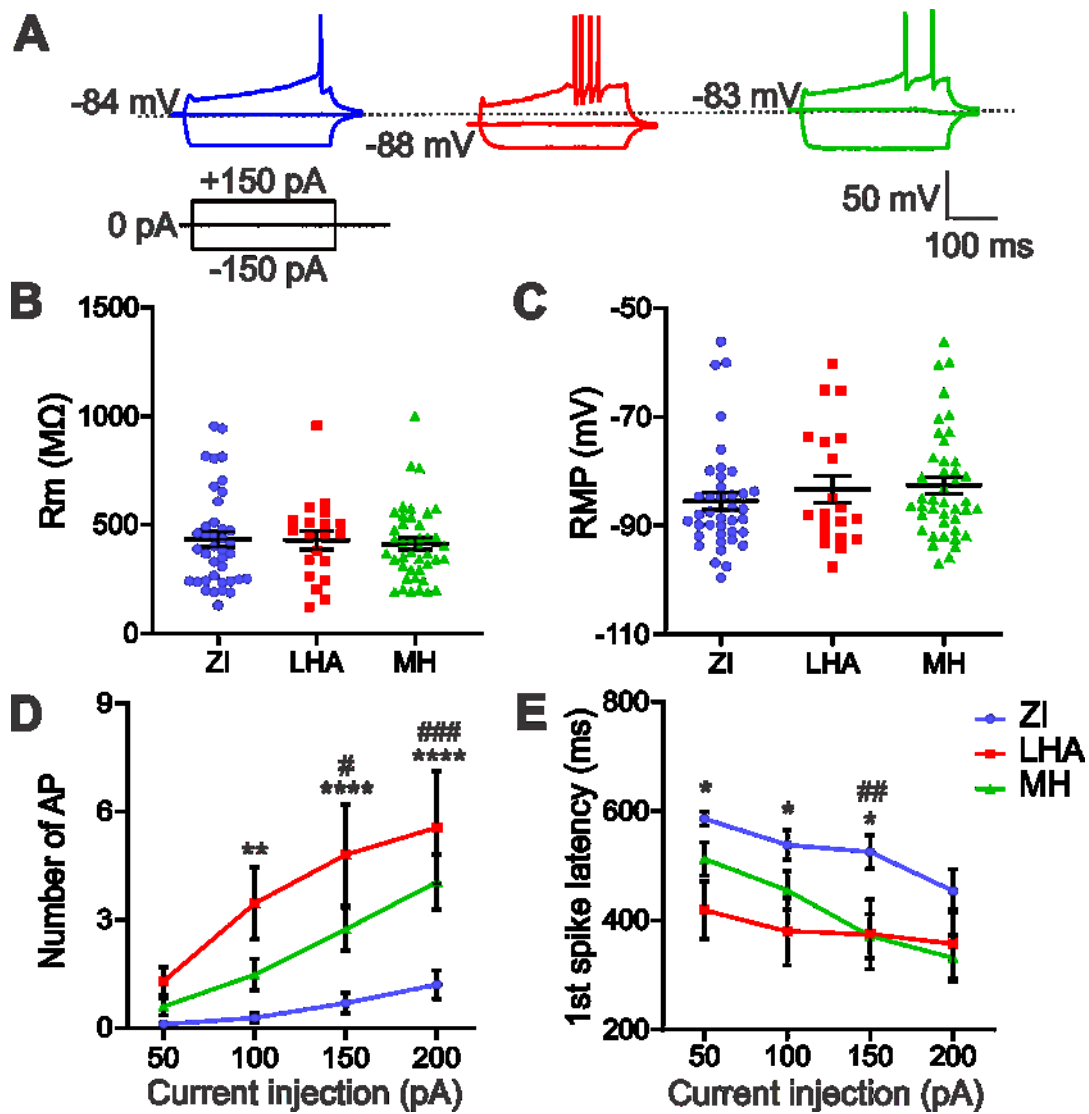


**Figure 5: Excitability of MCH neurons in distinct anatomical areas.**

(A) Representative current clamp recordings from MCH neurons in three different hypothalamic regions as indicated. ZI: zona incerta, LHA: lateral hypothalamic area and MH: medial hypothalamus

(B-C) Membrane resistance (Rm, B) and Resting membrane potential (RMP, C) of MCH neurons from the three hypothalamic areas.

(D-E) Number of AP spikes and (D) first spike latency (E) of MCH neurons during positive current injections.

Mean  $\pm$  SEM, one-way (B-C) and two-way (D-E) ANOVA with Tukey's post hoc comparisons: \* $p < 0.05$ , \*\* $p < 0.01$ , \*\*\* $p < 0.001$ , \*\*\*\* $p < 0.0001$  for ZI vs LHA; # $p < 0.05$ , ### $p < 0.01$ , #### $p < 0.001$  for ZI vs MH.

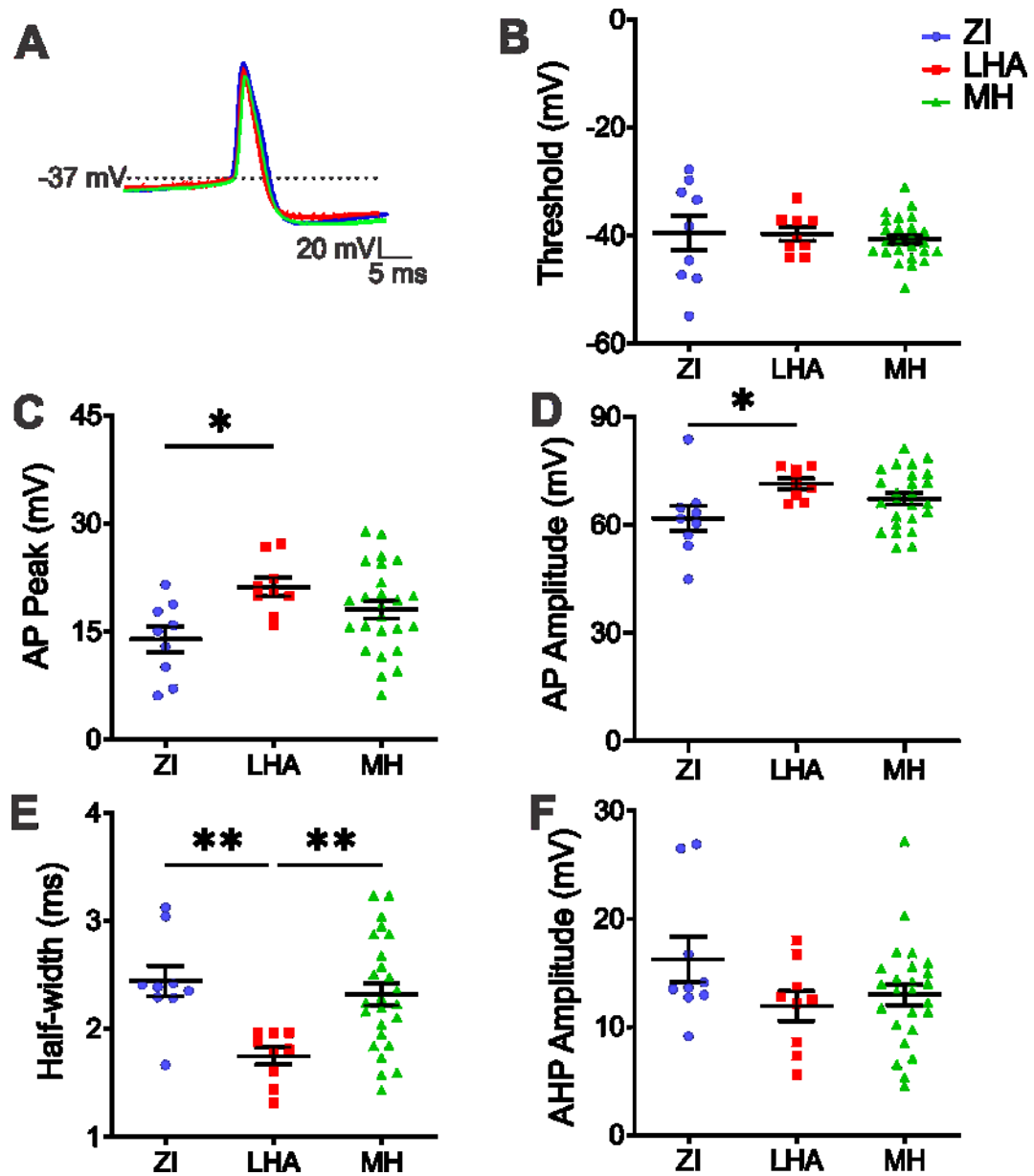


**Figure 6: Action potential (AP) waveform analysis of anatomical subpopulations of MCH neurons.**

(A) Averaged action potentials waveform recorded from MCH neurons in the zona incerta (ZI), lateral hypothalamic area (LHA) and medial hypothalamus. (B-F), AP waveform analysis of MCH neurons in the ZI, LHA and MH, including Threshold (B), AP peak (C), AP amplitude (D), Half-width (E) and AHP amplitude (F). Mean  $\pm$  SEM, \* $p < 0.05$ , \*\* $p < 0.01$ , one-way ANOVA with Tukey's post hoc test.

### 3.1.3 Genotype-dependent Differences in Excitability of Anatomical Subpopulations of MCH Neurons

Since both MCH-tdTomato and wildtype mice were used, it is possible that differences in excitability of MCH neurons exist in these mice. Due to the low sample size in the LHA from wildtype animals, however, statistical analyses could not be performed to test the effect of genotype (MCH-tdTomato: ZI n/N = 20/12, LHA n/N = 18/10, MH n/N = 24/14; wildtype: ZI n/N = 19/14, LHA n/N = 2/2, MH n/N = 18/12; Figure 7A- D). Similarly, statistical differences in the parameters of AP waveform could not be performed due to low sample size, particularly in LHA from wildtype mice (MCH-tdTomato: ZI n/N = 3/3, LHA n/N = 9/7, MHA n/N = 16/9; wildtype: ZI n/N = 7/7, LHA n = 0, MH n/N = 9/8). (Figures 8A-E). Nevertheless, there appears to be no obvious genotype-dependent differences based on visual inspection of the results.

It should be noted that, in addition to the difference in genotype, mice used in these experiments were bred at different facilities, namely the Memorial University Animal Services and purchased at Charles River. In addition, wildtype and transgenic mice have different background strains (wildtype: C57BL/6NCrl and MCH-cre/tdTomato: C57BL/6J). As such, parameters like breeding facilities, transport and background strain were also different between these groups of mice. However, the analysis above suggests that these factors did not have significant impact on the results.

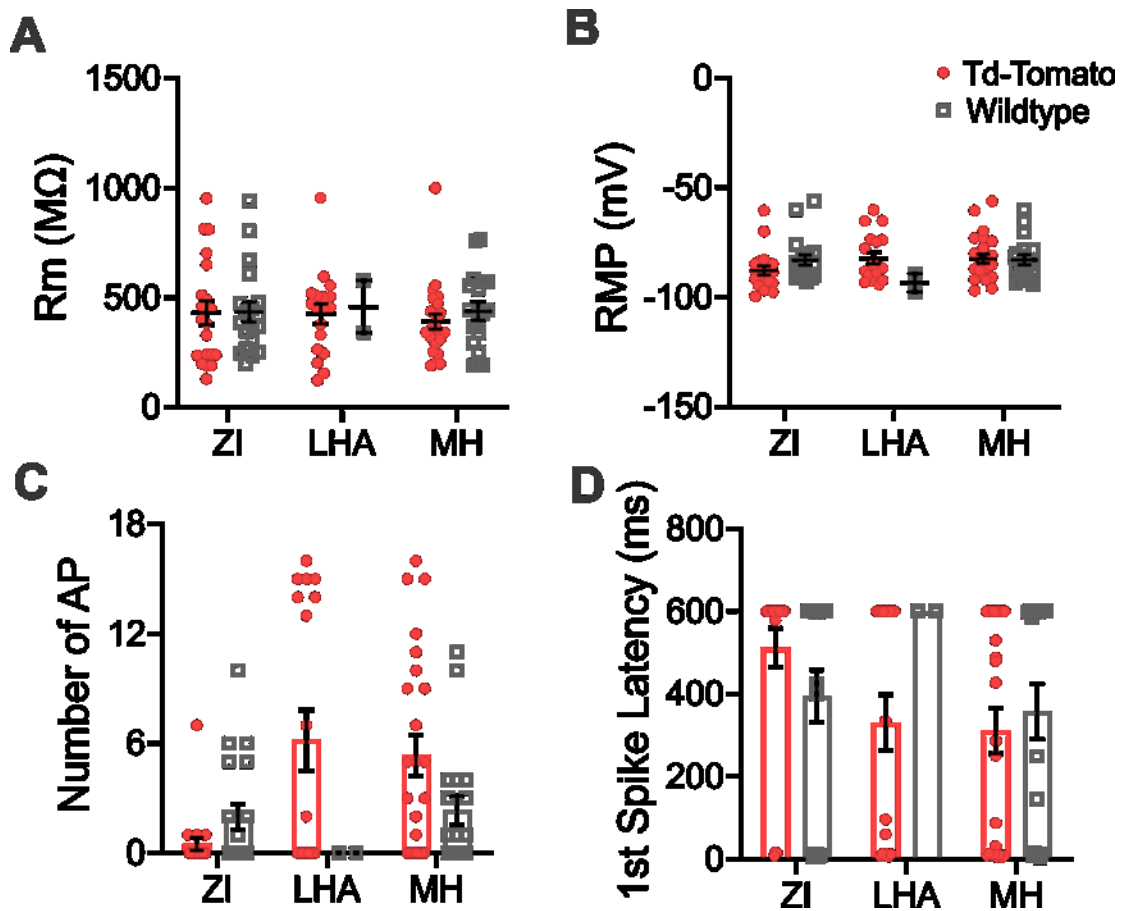


**Figure 7: Comparison of MCH neurons from td-Tomato and wildtype mice.**

(A) Representative current clamp recordings from MCH neurons in the ZI, LHA, and MH of tdTomato and wildtype mice.

(B) Resting membrane potential (RMP) of MCH neurons from the three anatomical areas display no genotypic differences.

(C-D) No genotypic differences in excitability for MCH neurons from MCH-tdTomato and wildtype mice in Number of AP (C) and First spike latency (D) at 200 pA current injection. *Mean ± SEM.*

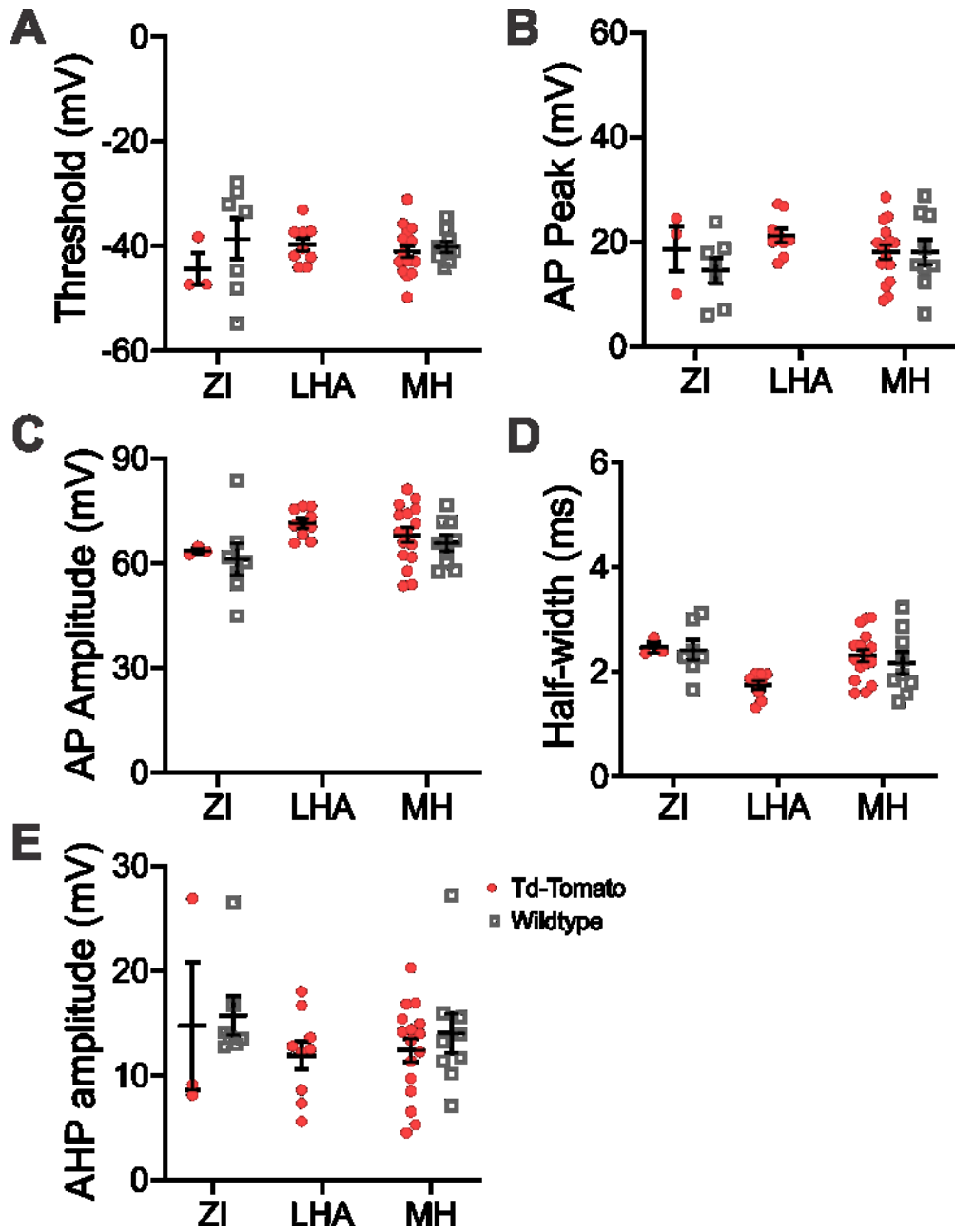


**Figure 8 : MCH neurons from td-Tomato and wildtype mice.**

(A-E): AP waveform analysis for MCH neurons from MCH-tdTomato and wildtype C57BL mice in the ZI, LHA and MH, including Threshold (A), AP peak (B), AP amplitude (C) Half-width (D) and, AHP amplitude (E). *Mean ± SEM*.

### 3.1.4 Excitability of Anatomical Area Subpopulations of MCH Neurons in Male and Female Mice

To determine whether area-specific differences in excitability of MCH neurons is influenced by the sex of the animals, the excitability and AP waveform of MCH neurons from the three anatomical areas from male and female mice were assessed (male ZI  $n/N = 24/17$ , LHA  $n/N = 8/6$ , MH  $n/N = 20/13$ ; female: ZI  $n/N = 6/4$ , LHA  $n/N = 8/4$ , MH  $n/N = 12/8$ ). There were no main effects of area or sex on membrane resistance, but there was significant interaction between area and sex ( $F_{2,72} = 6.980$ ,  $p = 0.0017$ ). Post hoc analysis showed no significant differences either (Figure 9B). There were no sex-dependent differences in RMP (main effect area:  $F_{2,72} = 2.063$ ,  $p = 0.1346$ ; main effect sex:  $F_{1,72} = 3.899$ ,  $P = 0.0521$ ; interaction:  $F_{2,72} = 0.1844$ ,  $p = 0.8320$ , two-way ANOVA; Figure 9A, C). On the other hand, analysis of number of AP showed a main effect of area ( $F_{2,72} = 7.508$ ,  $p = 0.0010$ , two-way ANOVA; Figure 9D), but there was no significant main effect of sex ( $F_{1,72} = 3.124$ ,  $p = 0.0814$ ) or interaction between sex of animals and anatomical area on number of AP ( $F_{2,72} = 2.459$ ,  $p = 0.0927$ ). Furthermore, there was no main effect of area, genotype or interaction effect of area and genotype on latency to first spike (two-way ANOVA: main effect area:  $F_{2,72} = 1.278$ ,  $p = 0.2849$ ; main effect sex:  $F_{1,72} = 1.044$ ,  $P = 0.3102$ ; interaction:  $F_{2,72} = 2.488$ ,  $p = 0.0902$ , Figure 9E).

With respect to AP waveform analysis, statistical differences in the parameters could not be performed due to low sample size of ZI and LHA MCH neurons that fired action potentials (male ZI  $n/N = 3/3$ , LHA  $n/N = 6/4$ , MH  $n/N = 10/7$ ; female: ZI  $n/N =$

2/2, LHA  $n/N = 2/2$ , MH  $n/N = 7/5$ ). Nonetheless, there appears to be no sex-dependent differences based on visual inspection of the results (Figures 10-E)

Together, these results suggests that the hypothalamic area-dependent differences in excitability observed in MCH neurons might be limited to just male mice. However, with the limited number of MCH neurons recorded in female mice, especially in the LHA, we cannot conclude female LHA MCH neurons are not as excitable as MCH neurons from male mice.

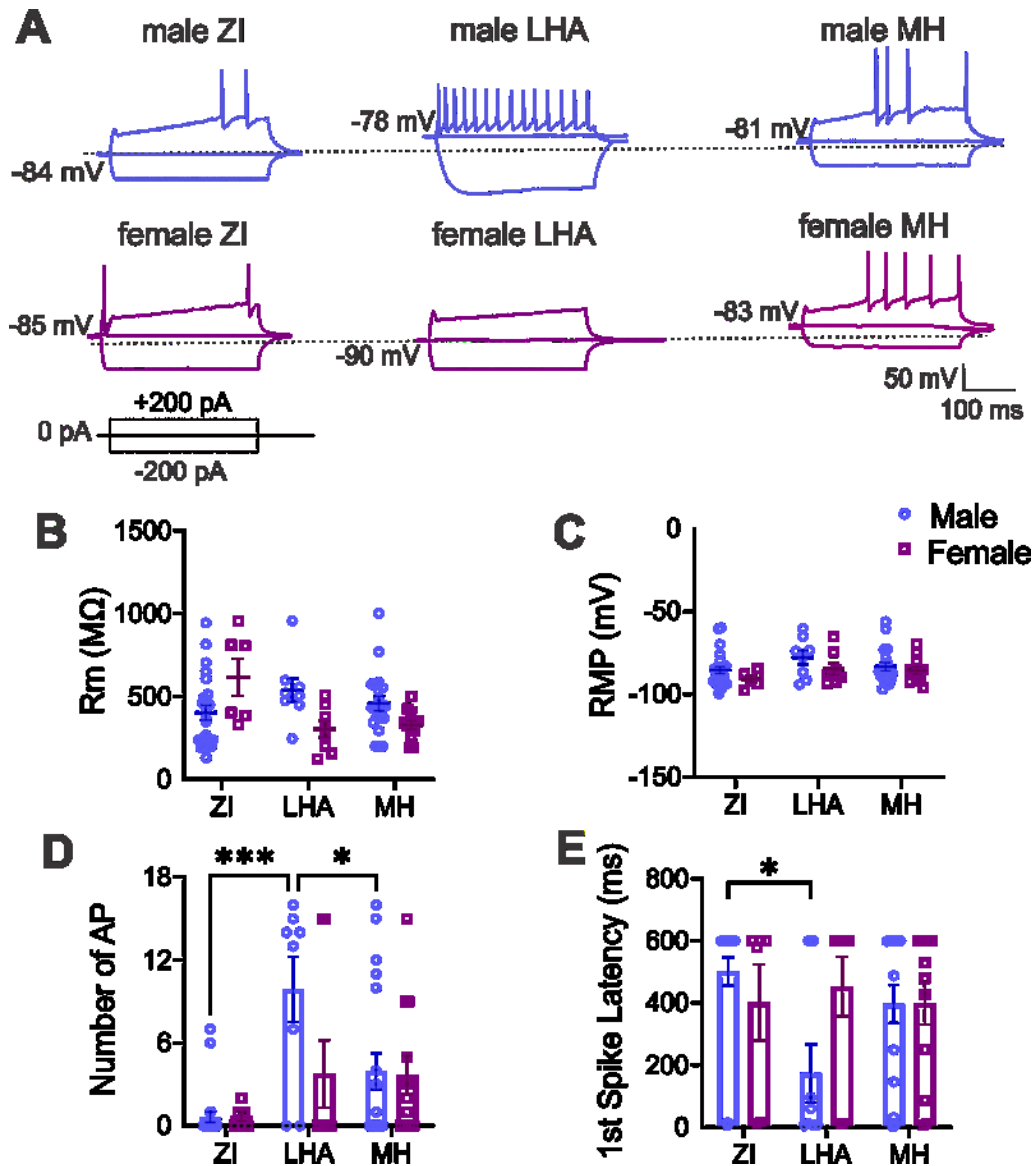


**Figure 9: Analysis for anatomical differences in MCH neurons from male and female mice.**

(A) Sample current clamp recordings from MCH neurons in the ZI, LHA, and MH from male and female mice. Notably, only 2 (of 8) MCH neurons in the LHA of female mice fired an AP, an MCH neuron with no AP is shown here.

(B-C) Membrane resistance ( $R_m$ , B) and resting membrane potential (RMP, C) of MCH neurons.

(D-E) Number of action potentials (D) and latency to first spike (E) in response to 200pA current injections.

Mean  $\pm$  SEM, \* $p < 0.05$ , \*\* $p < 0.01$ , \*\*\* $p < 0.001$ , \*\*\*\* $p < 0.0001$ , two-way ANOVA with post hoc comparisons.

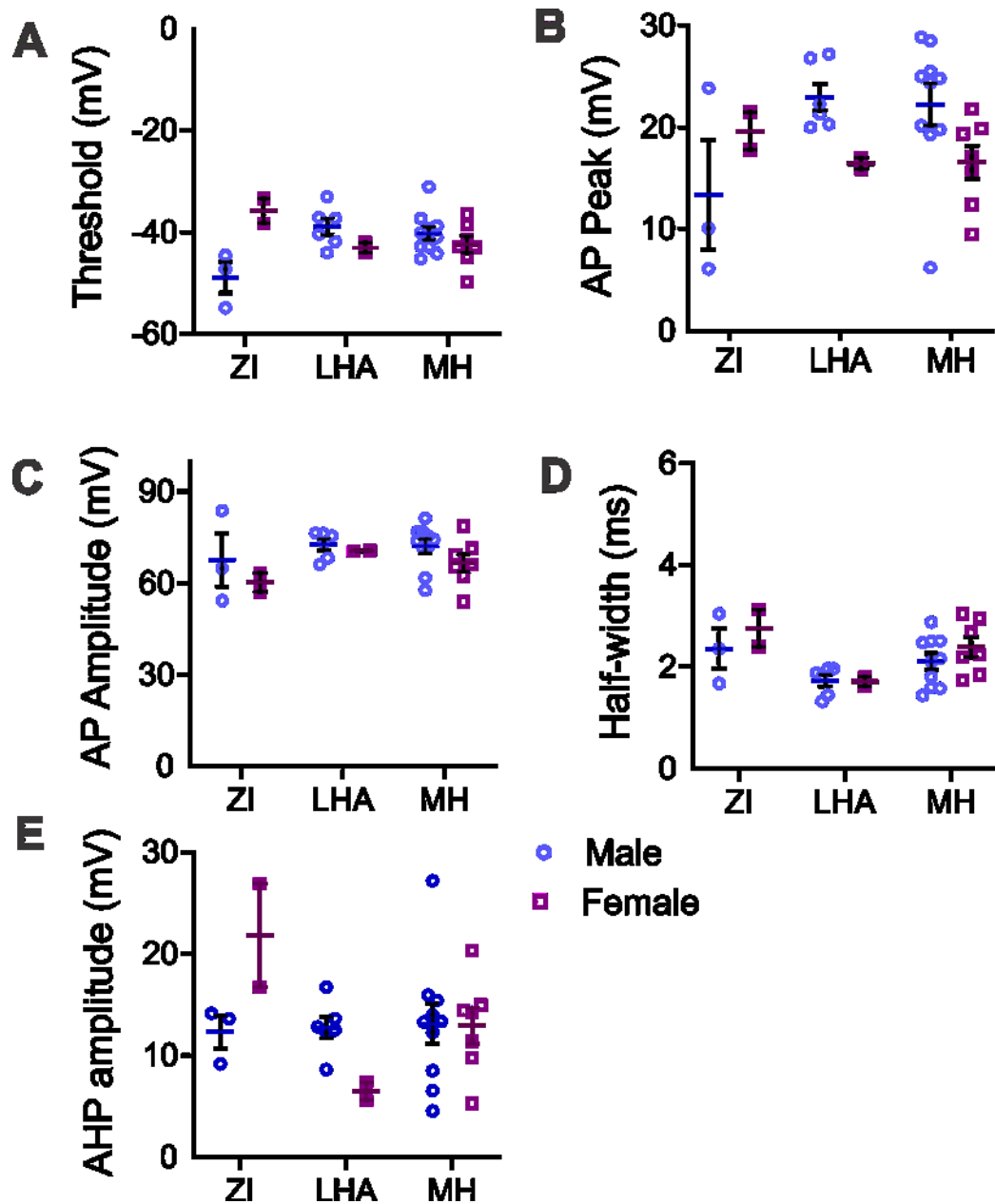


**Figure 10: Analysis of sexual dimorphism in AP properties of MCH neurons.**

(A-E): AP waveform analysis for MCH neurons from male and female mice in the ZI, LHA and MH, including Threshold (A), AP peak (B), AP amplitude (C) Half-width (D) and, AHP amplitude (E). Mean  $\pm$  SEM.

### 3.1.5 Excitability of MCH Neurons from Different Anatomical Areas Held at

#### Subthreshold Potential

With positive current injections, many of the MCH neurons assessed fired at least one AP. However, a good proportion of cells did not fire AP, even with maximum positive current injection (Figure 4A, B). These silent cells could not be included to assess AP waveform parameters, which could have skewed the results. Therefore, a subset of MCH neurons that did not fire an AP with maximum current injection were held at a subthreshold potential and their excitability and AP waveform properties were analysed (ZI  $n/N = 8/7$ , LHA  $n/N = 11/7$ , MH  $n/N = 9/8$ ). There was no significant difference in membrane resistance among the three areas ( $F_{2,26} = 0.6047$ ,  $p = 0.5538$ ; Figure 11B). With respect to number of AP, a two-way ANOVA showed a significant main effect for positive current injection ( $F_{3,78} = 106.8$ ,  $p < 0.0001$ ), whereas the main effect of anatomical area was non-significant ( $F_{2,26} = 3.269$ ,  $p = 0.0542$ ). However, the interaction effect between area and amount of current injection was significant ( $F_{6,78} = 5.071$ ,  $p = 0.0002$ ). Tukey post hoc comparisons indicated that with higher current injections, LHA and MH MCH neurons fired more action potentials than ZI MCH neurons (Figure 11A, C). Analysis of first spike latency showed a significant main effect of positive current injection on time to first spike ( $F_{3,78} = 53.27$ ,  $p < 0.0001$ ), while the main effect of anatomical area on first spike latency was not significant ( $F_{2,26} = 0.6987$ ,  $p = 0.5063$ ). There was no significant interaction between positive current and area ( $F_{6,78} = 1.260$ ,  $p = 0.2854$ ; Figure 11A, D).

The AP waveform analysis showed differences in threshold ( $p = 0.0144$ , one-way ANOVA; Figure 12A) with ZI MCH neurons displaying higher threshold to fire than MCH neurons in LHA and MH. Similarly, there was significant area-dependent main effect differences observed in AP peak ( $p = 0.0355$ , one-way ANOVA; Figure 12B), although post-hoc multiple comparison showed no significant difference between groups ( $p > 0.05$ ). Nonetheless, AP amplitude showed a significant difference between areas ( $p = 0.0279$ , one-way ANOVA; Figure 12C). No differences were noted in half-width ( $p = 0.0615$ , one-way ANOVA; Figure 12D) and AHP amplitude ( $p = 0.2343$ , one-way ANOVA; Figure 12E).

These results indicate there may be differences in the excitability of brain area specific MCH subpopulations.

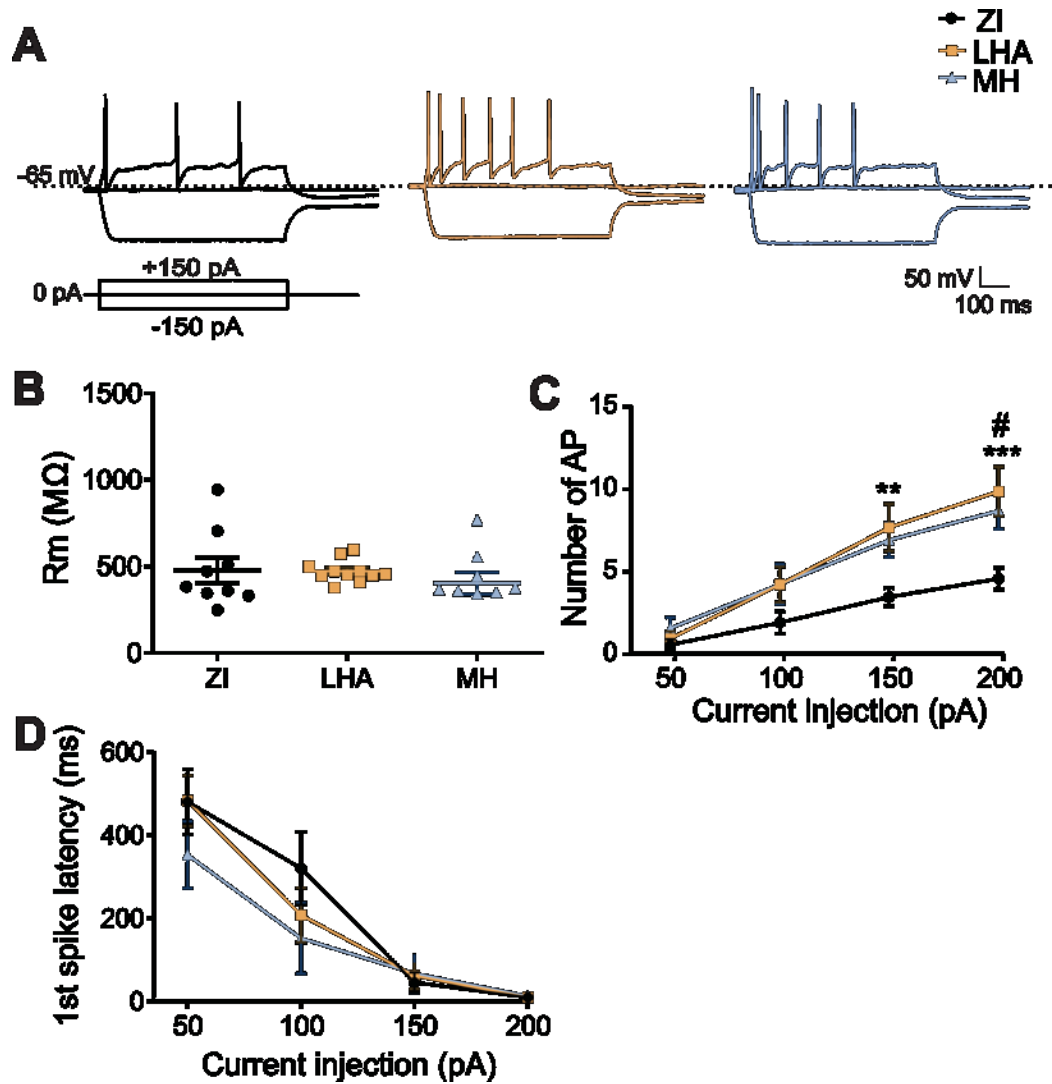


**Figure 11: MCH neurons from different anatomical areas held at subthreshold potential.**

(A) Representative current clamp recordings from MCH neurons in the ZI, LHA, and MH held at subthreshold potential.

(B-C) Number of action potentials (C) and latency to first spike in response to various current injections.

Data is mean  $\pm$  SEM, one-way (B) and two-way ANOVA (C-D) with post hoc comparisons: \*\* $p < 0.01$ , \*\*\* $p < 0.001$ , for ZI vs LHA; # $p < 0.05$  for ZI vs MH.

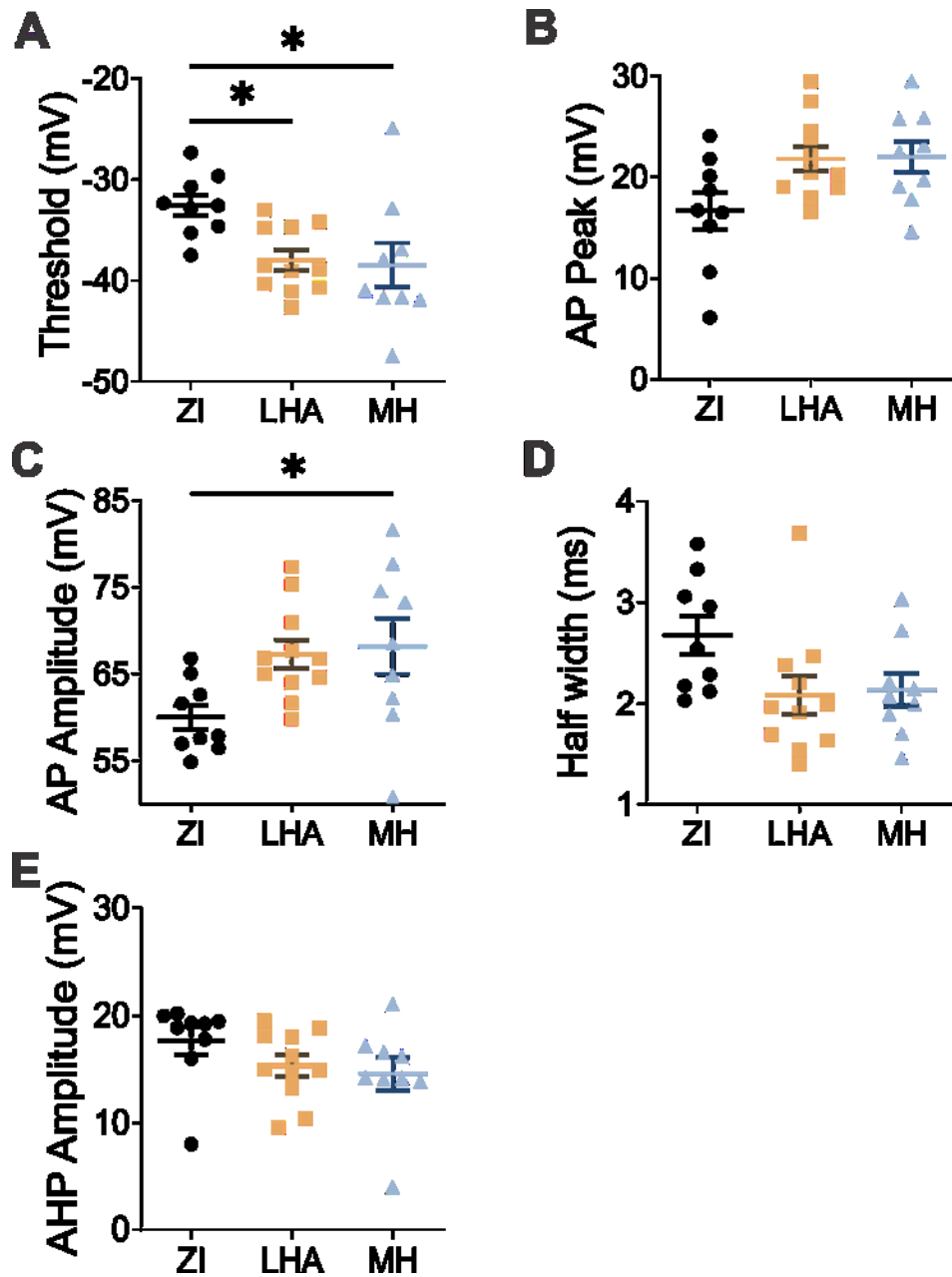


**Figure 12: Electrophysiological properties of MCH neurons held at a subthreshold potential.**

(A) Averaged action potentials waveform recorded from MCH neurons in the zona incerta (ZI), lateral hypothalamic area (LHA) and medial hypothalamus.

(B-F) AP waveform analysis for MCH neurons in the ZI, LHA and MH, including Threshold (B), AP peak (C), AP amplitude (D), Half-width (E) and AHP amplitude (F).

\* $p < 0.05$ ,  $Mean \pm SEM$ .

## 3.2 Neurochemical Subpopulations of MCH Neurons

### 3.2.1 Excitability of Neurochemical Subpopulations of MCH Neurons

Another way to classify MCH neurons is by the co-expression of another neuropeptide CART. First, the electrophysiological properties of MCH neurons were determined according to their co-expression of CART, regardless of their anatomical localization (Figure 13A, B). No difference was observed in the membrane resistance between the two neurochemical subpopulations of MCH neurons (MCH+/CART+  $n/N = 51/28$ , MCH+/CART-  $n/N = 7/6$ ,  $p = 0.4289$ , unpaired t-test; Figure 14B). Compared to MCH+/CART+ neurons, MCH+/CART- neurons had a depolarized RMP ( $p = 0.0187$ , unpaired t-test; Figure 14A, C). It was noted by visual inspection that majority of MCH+/CART- neurons displayed an H-current during hyperpolarizing current injection. Consequently, the H-current amplitude was analyzed at -200 pA current injection where H-current was most prominent, which found a significant difference between the two groups ( $p = 0.0016$ , Mann-Whitney test; Figure 14A, D).

Number of APs and latency to first spike were analyzed with 2-way ANOVA. The main effect of positive current injection ( $F_{3,168} = 45.50$ ,  $p < 0.0001$ ) and the cell type (i.e., CART expression) on number of APs were significant ( $F_{1,56} = 29.99$ ,  $p < 0.0001$ ). There was also a significant interaction between positive current injection and CART expression ( $F_{3,168} = 20.29$ ,  $p < 0.0001$ ). Sidak's multiple comparisons test showed that with increasing positive current injection, MCH+/CART- cells fired more APs than MCH+/CART+ neurons (Figure 14E). In analysis of latency to first spike, there was a significant main effect of

CART expression ( $F_{1,56} = 15.08$ ;  $p = 0.0003$ ) and current injection ( $F_{3,168} = 3.452$ ,  $p = 0.0179$ ; Figure 14F), while there was no significant interaction between current injection and CART expression ( $P = 0.7666$ ).

AP waveform analysis revealed no significant differences in any of the parameters analysed (MCH+/CART+  $n/N = 18/13$ , MCH+/CART-  $n/N = 5/4$ ) including threshold ( $p = 0.0560$ , unpaired t-test; Figure 15B), AP peak ( $p = 0.1962$ ; unpaired t-test; Figure 15C), AP amplitude ( $p = 0.3611$ , unpaired t-test; Figure 15D), half-width ( $p = 0.0918$ , unpaired t-test; Figure 15E) and AHP amplitude ( $p = 0.2913$ , unpaired t-test; Figure 15F).

Taken together, these results suggest that there may be neurochemical subpopulations of MCH neurons with distinct electrophysiological properties. Specifically, MCH neurons that do not co-express CART are more excitable than CART co-expressing MCH neurons.

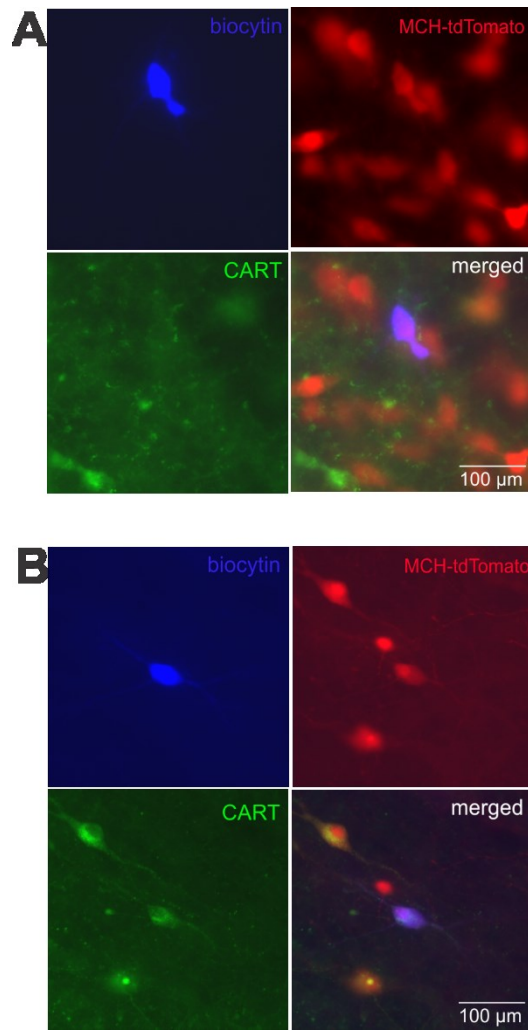


**Figure 13: Post hoc immuno-histochemical confirmation of MCH and CART co-expression.**

- (A) Sample image of CART-immunonegative MCH neuron (MCH+ CART-) from a tdTomato mouse. The biocytin-labeled cell (blue) is a tdTomato-MCH neuron (red) that is immunonegative for CART (green), confirmed by the merged image.
- (B) Sample image of CART-immunopositive MCH neuron (MCH+ CART+) from a tdTomato mouse. The biocytin-labeled cell (blue) is a tdTomato-MCH neuron (red) that is immunopositive for CART (green), confirmed by the merged image.

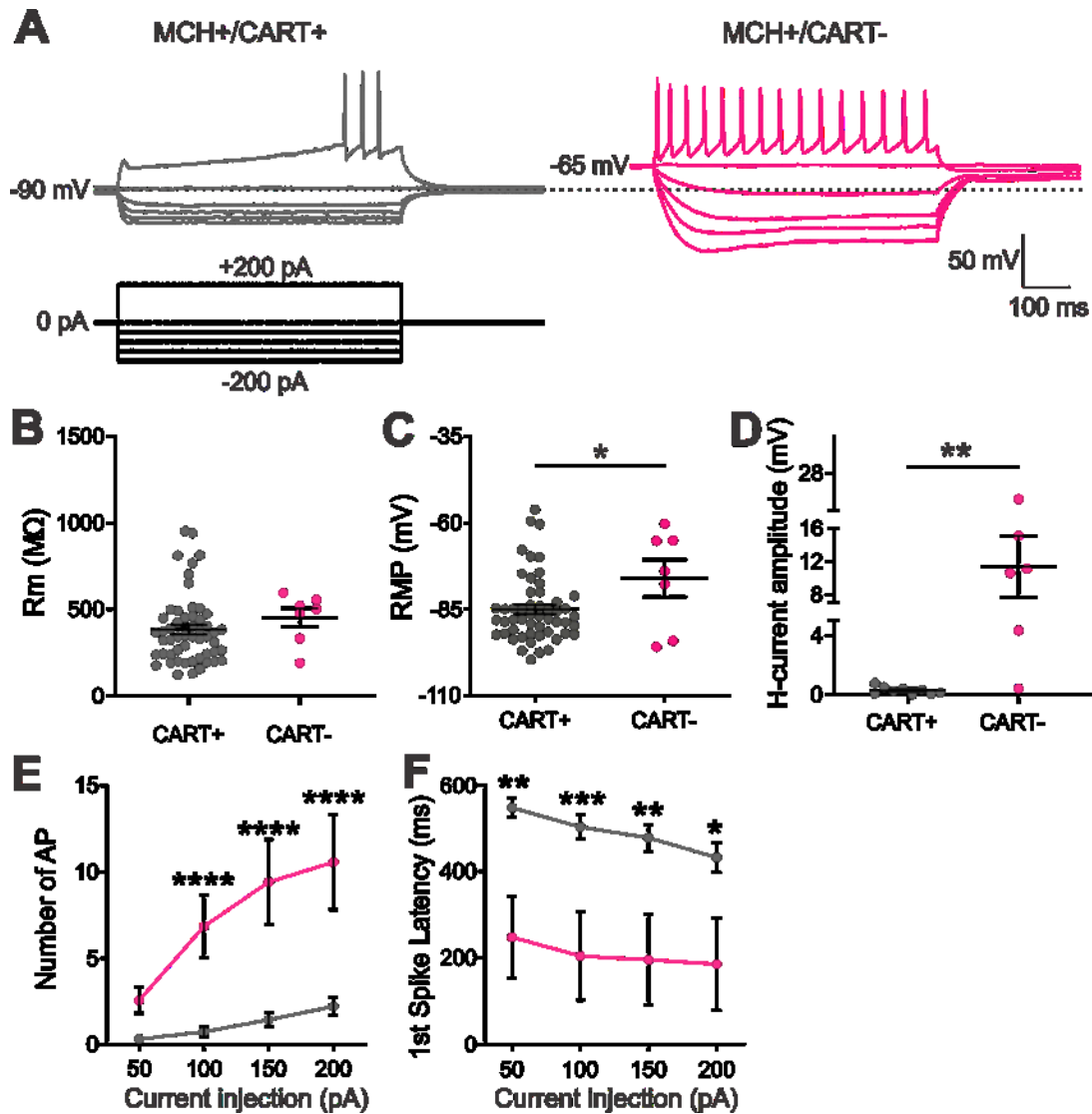


**Figure 14: MCH neurons display neurochemical differences in excitability.**

(A) Representative current clamp recordings from MCH+/CART+ and MCH+/CART- neurons.

(B) Membrane resistance of MCH+/CART+ and MCH+/CART- neurons.

(C) Resting membrane potential (RMP) of MCH+/CART+ and MCH+/CART- neurons.

(D) H-current amplitude of MCH neurons from MCH+/CART+ and MCH+/CART- neurons with 200 pA current injection.

(E-F) Number of Action potentials (E), and first spike latency (F) of neurochemical subpopulation of MCH neurons during positive current injections.

\* $p < 0.05$ , unpaired t-test for RMP and H-current amplitude. \* $p < 0.05$ , \*\* $p < 0.01$ , \*\*\* $p < 0.001$ , \*\*\*\* $p < 0.0001$ , two-way ANOVA with Sidak post-test, Mean  $\pm$  SEM.

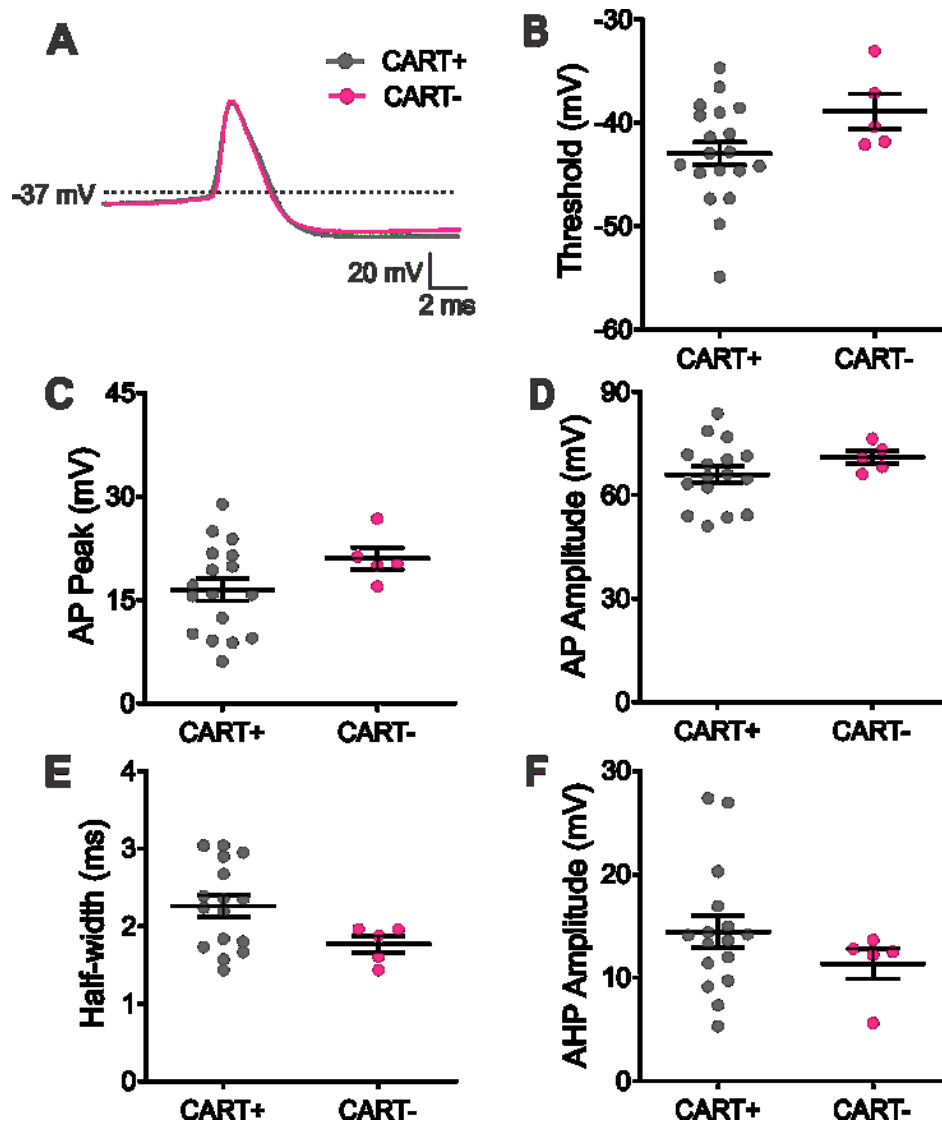


**Figure 15: Action potential waveform analysis in neurochemical subpopulations of MCH neurons.**

(A) Averaged action potentials waveform recorded from MCH+/CART+ and MCH+/CART- neurons.

(B-F) AP waveform analysis for CART expressing and non-expressing MCH neurons including threshold (B), AP peak (C), AP amplitude (D), half-width (E), and AHP amplitude (F). *Mean ± SEM*.

### 3.2.2 Excitability of Neurochemical Subpopulations of MCH Neurons in Male and Female Mice

The present study included MCH neurons from both sexes, which could have affected the results. However, there was a low number of MCH+*CART*<sup>-</sup> from female mice to reliably assess if there were any sex-dependent differences (*CART*<sup>+</sup>: male  $n = 27/15$ , female  $n = 28/13$ ; *CART*<sup>-</sup>: male  $n = 7/6$ , female  $n = 2/2$ ). Therefore, we assessed the excitability and AP waveform parameters of MCH+/*CART*<sup>+</sup> and MCH+/*CART*<sup>-</sup> within male mice only. There were no significant differences in membrane resistance ( $p = 0.2565$ , *t*-test; Figure 16B) between MCH+/*CART*<sup>+</sup> and MCH+/*CART*<sup>-</sup> neurons from male mice. In contrast, the RMP was more depolarized ( $p = 0.0247$ , *t*-test; Figure 16C) and the H-current amplitude was greater in MCH+/*CART*<sup>-</sup> than in MCH+/*CART*<sup>+</sup> neurons from male mice ( $p = 0.0043$ , Mann-Whitney test; Figure 16D). Furthermore, the number of APs and latency to first spike revealed cell type-specific differences (Figure 16E, F). Specifically, 2-way ANOVA analysis showed a significant main effect of positive current injection ( $F_{1,42} = 61.76$ ,  $p < 0.0001$ ) and *CART* expression ( $F_{1,31} = 51.43$ ,  $p < 0.0001$ ) on number of APs, and a significant interaction between current injection and *CART* expression within male MCH neurons ( $F_{3,93} = 39.75$ ,  $p < 0.0001$ ). Sidak's post hoc comparisons revealed that with more depolarizing current injections, MCH+/*CART*<sup>-</sup> neurons from male mice fired more APs than MCH+/*CART*<sup>+</sup> neurons (Figure 16E). With respect to first spike latency, there was significant main effect of *CART* expression ( $F_{1,31} = 19.65$ ,  $p = 0.0001$ ) and current injection ( $F_{1.7, 51.40} = 4.023$ ,  $p = 0.0304$ ), however there was no significant interaction

effect between CART expression and depolarizing current ( $F_{3, 93} = 0.5349$ ,  $p = 0.6595$ ) indicating that the difference in first spike latency between CART+ and CART- male MCH neurons is not dependent on amount of current injected (Figure 16F).

AP waveform analysis revealed no differences in any of the parameters analysed within male mice (MCH+/CART+  $n = 6/6$ ; MCH+/CART-  $n = 5/4$ ) including threshold ( $p = 0.2187$ , t-test; Figure 17A), AP peak ( $p = 0.8549$ , t-test; Figure 17B), AP amplitude ( $p = 0.9646$ , t-test; Figure 17C), half-width ( $p = 0.3941$ , t-test; Figure 17D) and AHP amplitude ( $p = 0.8763$ , Mann-Whitney test; Figure 17E). These results suggest that the difference in excitability and the presence of H-current observed between neurochemical subpopulations of MCH neurons are present in male animals. This should be confirmed with female MCH neurons in the future with a larger sample size.

Next, we assessed if there were any sex-dependent differences in CART+ MCH neurons, since there was sufficient sample size for from both male and female mice (CART+: male  $n/N = 27/15$ , female  $n/N = 28/13$ ). There were no significant sex-dependent differences in any of the parameters analysed: membrane resistance ( $p = 0.6259$ , t-test; Figure 18A), RMP ( $p = 0.7567$ , t-test; Figure 18B). With respect to number of AP, there was no main effect of sex ( $F_{1,53} = 1.875$ ,  $p = 0.1766$ ) but there was main effect of current injection as expected ( $F_{1,159} = 20.88$ ,  $p < 0.0001$ ) and significant interaction between sex of the animal and current injection ( $F_{1,159} = 3.874$ ,  $p < 0.0104$ ). Sidak's post hoc multiple comparison revealed no significant differences (Figure 18C). First spike latency, showed significant main effect of sex ( $F_{1,212} = 5.871$ ,  $p = 0.0162$ ) and

current injection ( $F_{3, 212} = 3.786$ ,  $p = 0.0112$ ), however there was no significant interaction effect between sex of mice and depolarizing current ( $F_{3, 93} = 0.5349$ ,  $p = 0.6595$ ) indicating that the difference in first spike latency between male and female MCH -positive neurons is not dependent on amount of current injected (Figure 18D).

AP waveform analysis also revealed no differences in any of the parameters analysed within CART-positive male and female mice (male  $n/N = 7/6$ ; female  $n/N = 12/7$ ) including threshold ( $p = 0.3247$ , t-test; Figure 19A), AP peak ( $p = 0.5096$ , t-test; Figure 19B), AP amplitude ( $p = 0.5468$ , t-test; Figure 19C), half-width ( $p = 0.4731$ , t-test; Figure 19D) and AHP amplitude ( $p = 0.8413$ , t-test; Figure 19E). These results suggest that the difference in excitability and the presence of H-current observed between neurochemical subpopulations of MCH neurons may not be due to the sex of the animal.

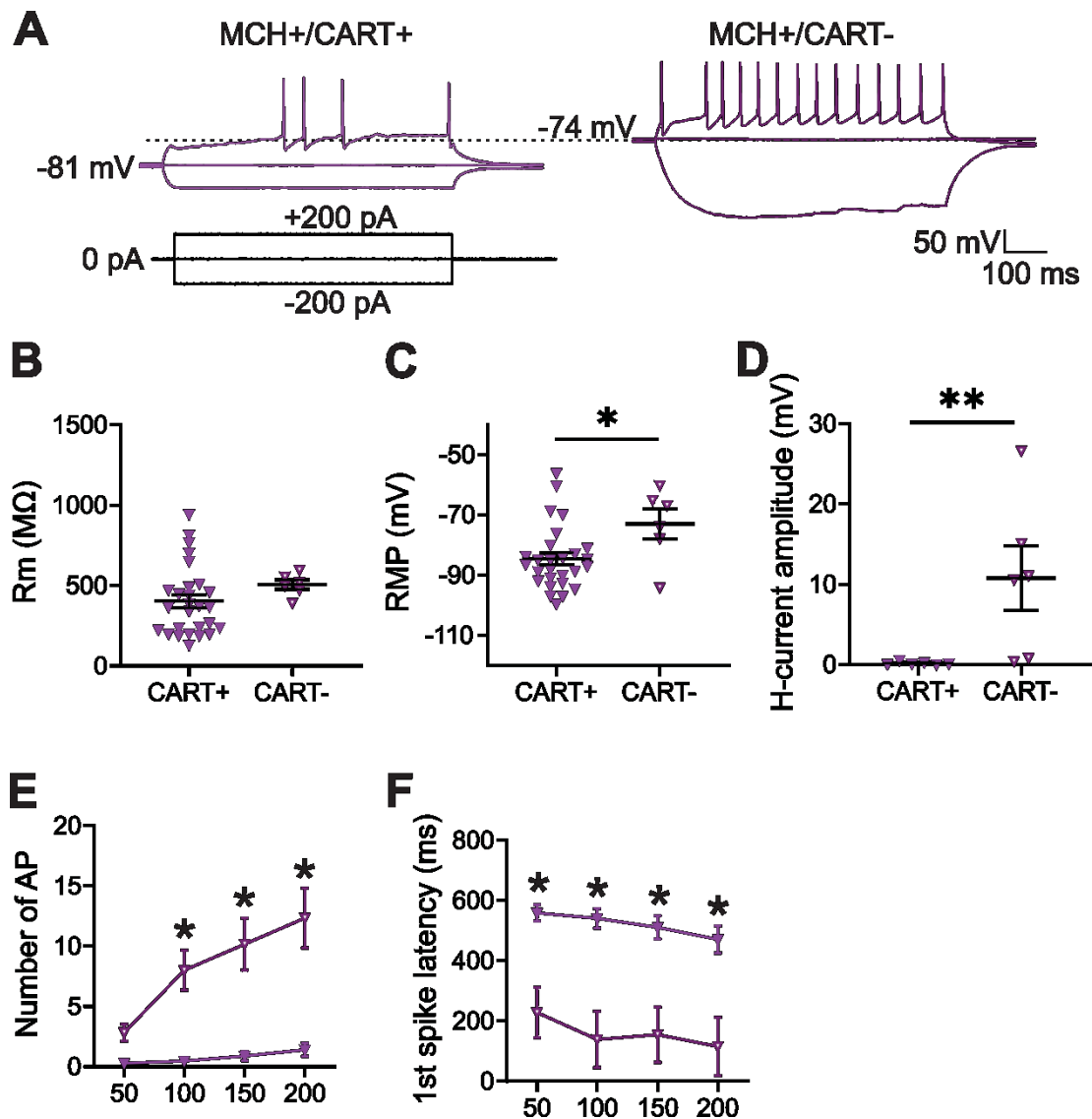


**Figure 16: Characteristics of MCH neurons with or without CART co-expression in male mice.**

(A) Representative current clamp recordings from MCH neurons from MCH+/CART+ and MCH+/CART- male mice.

(B-D) Membrane resistance (Rm, B), resting membrane potential (RMP, C) and H-current amplitude (D) of MCH neurons.

(E-F) Number of action potentials (D) and latency to first spike (E) in response to 200pA current injections. Need a symbol legend for E and F

\* $p < 0.05$ , \*\* $p < 0.01$ , \*\*\* $p < 0.001$ , \*\*\*\* $p < 0.0001$ , unpaired *t*-test (D) and two-way ANOVA (E-F). Mean  $\pm$  SEM.

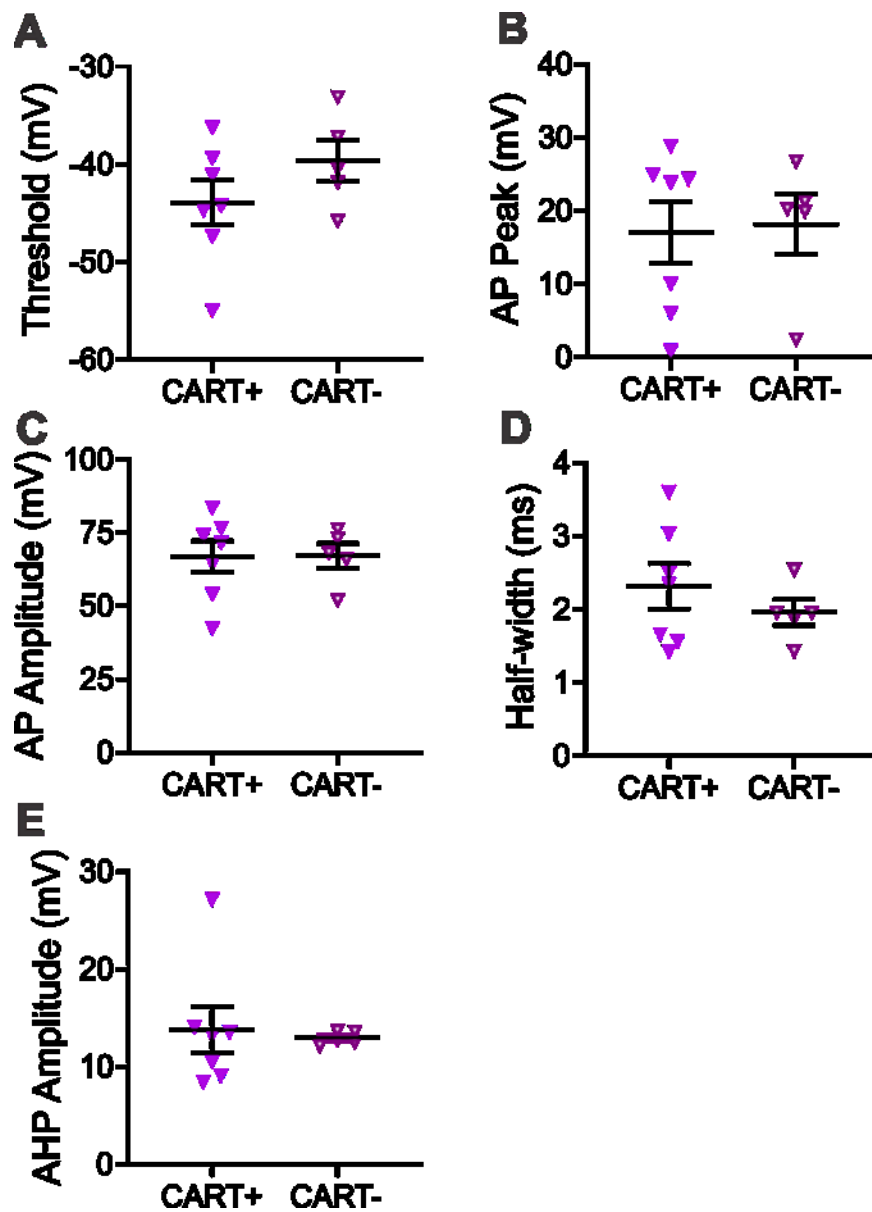


Figure 17: AP waveform analysis of neurochemical subpopulations of MCH from male mice.

(A-E) Various parameters of AP waveform including Threshold (A), Action potential (AP) peak (B), AP amplitude (C), half-width (D), and After-hyperpolarizing potential (AHP, E) of MCH+/CART+ and MCH+/CART- neurons from male mice. *Mean ± SEM*.

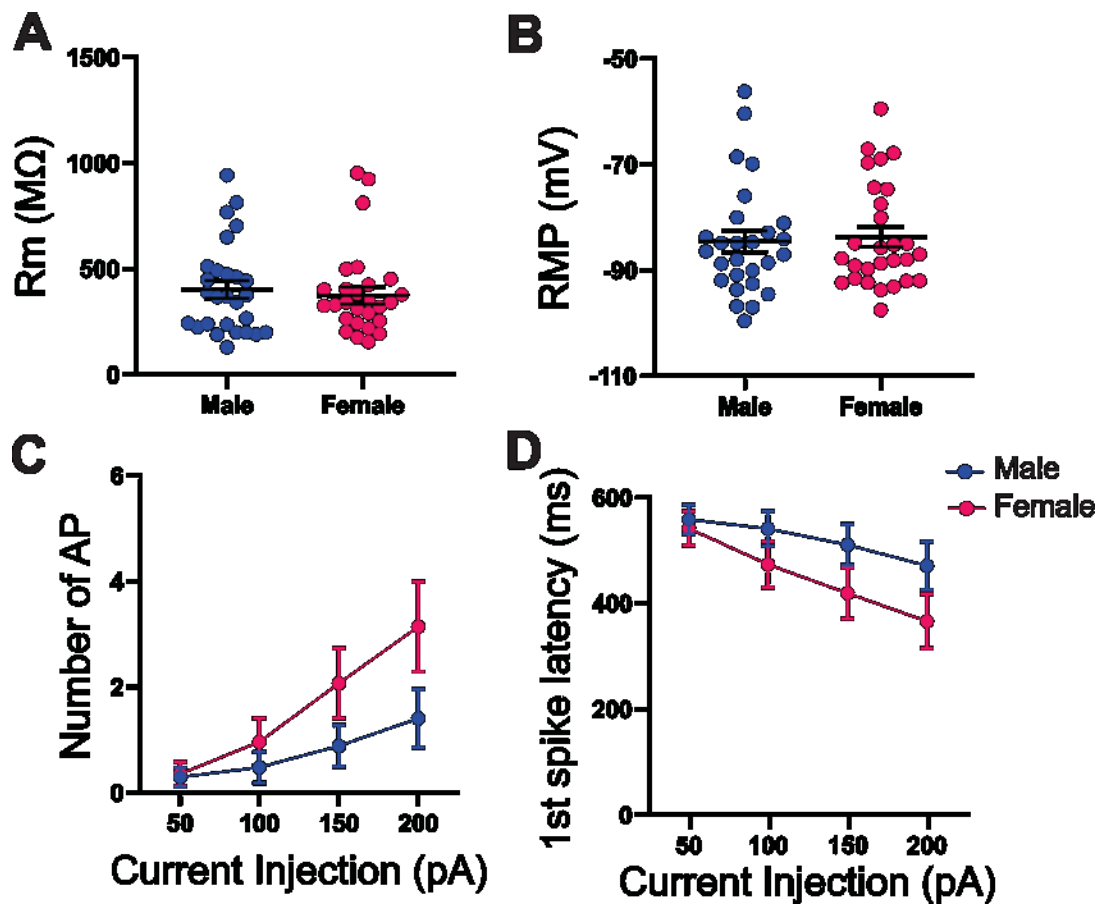


Figure 18: Analysis of sexual dimorphism in excitability of CART-expressing MCH neurons

(A-B) Membrane resistance ( $R_m$ , A), resting membrane potential (RMP, B) of MCH neurons.

(C-D) Number of action potentials (C) and latency to first spike (D) in response to 200pA current injections.

Error bar:  $Mean \pm SEM$ .

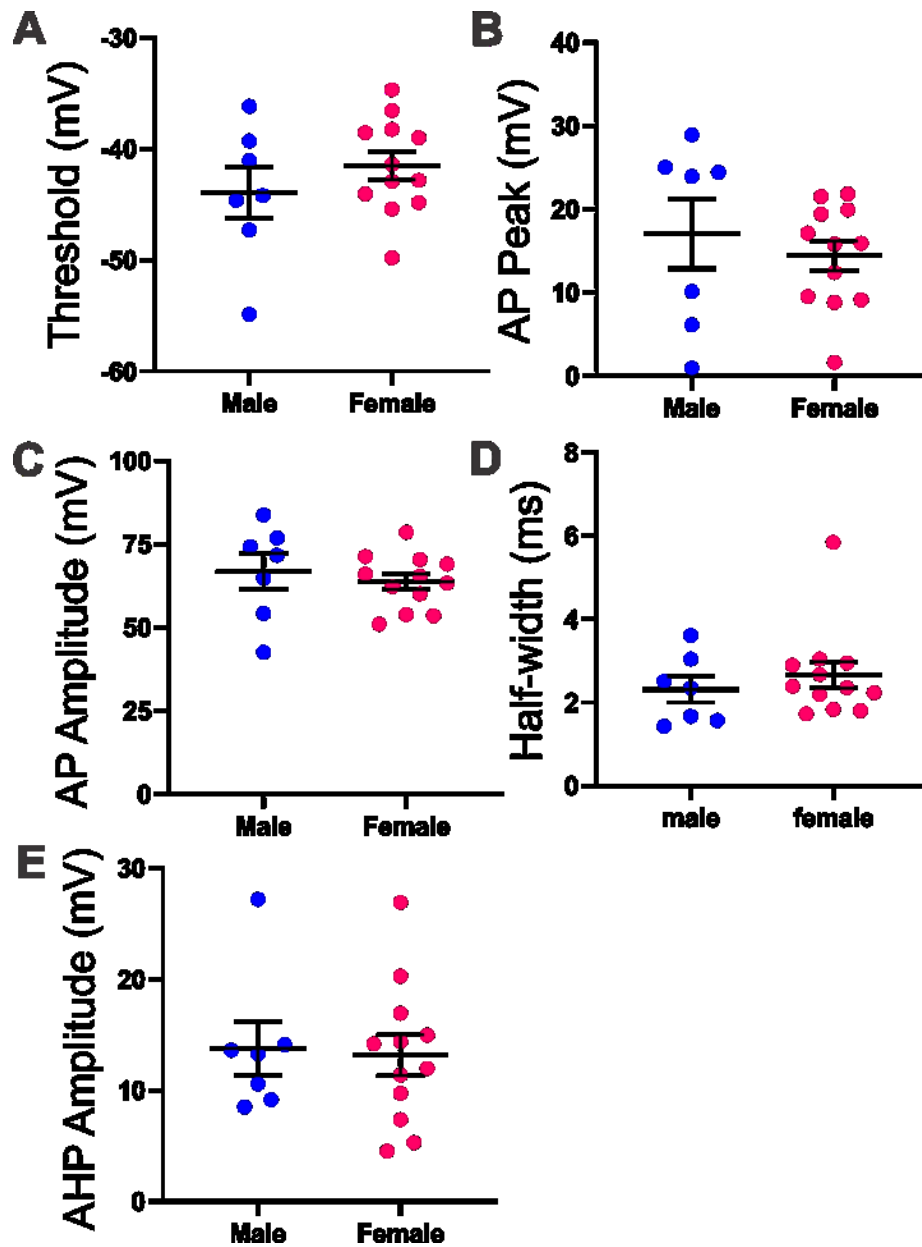


Figure 19: AP waveform analysis for sex-dependent differences in CART-expressing MCH neurons.

(A-E) Various parameters of AP waveform including Threshold (A), Action potential (AP) peak (B), AP amplitude (C), half-width (D), and After-hyperpolarizing potential (AHP, E) of MCH+/CART+ and MCH+/-CART- neurons from male mice. *Mean  $\pm$  SEM.*

### **3.3 Anatomical Distribution of MCH and CART Expression in the Mouse**

#### **Hypothalamus**

The specific distribution of MCH neurons and their colocalization with CART were analyzed using double immunostaining for MCH and CART. MCH neurons were distributed throughout the hypothalamus including the LHA, ZI, and MH (Figure 20A). CART expression was found to be localized in similar regions as MCH neurons i.e., in the LHA, MH and ZI (Figure 20A). However, some regional differences were found, with most of the MCH+/CART+ neurons observed in the ZI and MH, with fewer double staining observed in the LHA (Figure 20A). In fact, the LHA had the majority of MCH+/CART- neurons, with few or no MCH+/CART- neurons in the ZI and MH ( $p < 0.0001$ , Chi-square test; Figure 20B).

#### **3.3.1 Excitability of Neurochemical Subpopulations of MCH Neurons in Distinct**

##### **Hypothalamic Areas**

Many MCH neurons were observed in the ZI, LHA and MH (Figure 20). Comparably, most MCH neurons recorded for electrophysiological assessment co-localized CART in the ZI (26 of 26 neurons) and MH (22 of 23 neurons), while LHA had equal proportion of MCH+/CART+ (7 of 14 neurons) and MCH+/CART- neurons (7 of 14 cells). Consequently, region-specific electrophysiological properties were analyzed only for MCH+/CART+ neurons within the ZI, LHA and MH.

Among these areas, there were no differences observed in the membrane resistance (ZI  $n/N = 23/14$ , LHA  $n/N = 7/3$ , MH  $n/N = 22/14$ ,  $p = 0.3093$ , one-way ANOVA, Kruskal-Wallis test; Figure 21B) and RMP ( $p = 0.7280$ , one-way ANOVA; Figure 21A, C). Two-way ANOVA comparison for the effect of depolarizing current injection and anatomical area on number of AP showed significant main effect of driving current as expected ( $F_{3,156} = 15.45$ ,  $p < 0.0001$ ), while there was no significant main effect of area ( $F_{2,52} = 1.957$ ,  $P = 0.1516$ ) or interaction between amount of current injected and anatomical area on number of AP ( $F_{6,156} = 1.781$ ,  $p = 0.1063$ ; Figure 21D). Similarly, there was a significant main effect of driving current on first spike latency ( $F_{3,156} = 6.097$ ,  $p = 0.0006$ ). However, there was neither a main effect of anatomical area ( $F_{2,52} = 2.005$ ,  $P = 0.1450$ ) nor interaction of anatomical area and current injection ( $F_{6,156} = 0.7895$ ,  $p = 0.5794$ ) on first spike latency (Figure 21E). AP waveform analysis could not be performed due to low sample size (ZI  $n/N = 5/4$ , LHA  $n/N = 1/1$ , MH  $n/N = 13/6$ ; Figures 22A-E).

Together, these results indicate that the anatomical location of CART+ MCH neurons does not correlate with distinct electrophysiological properties of MCH+/CART+ neurons.

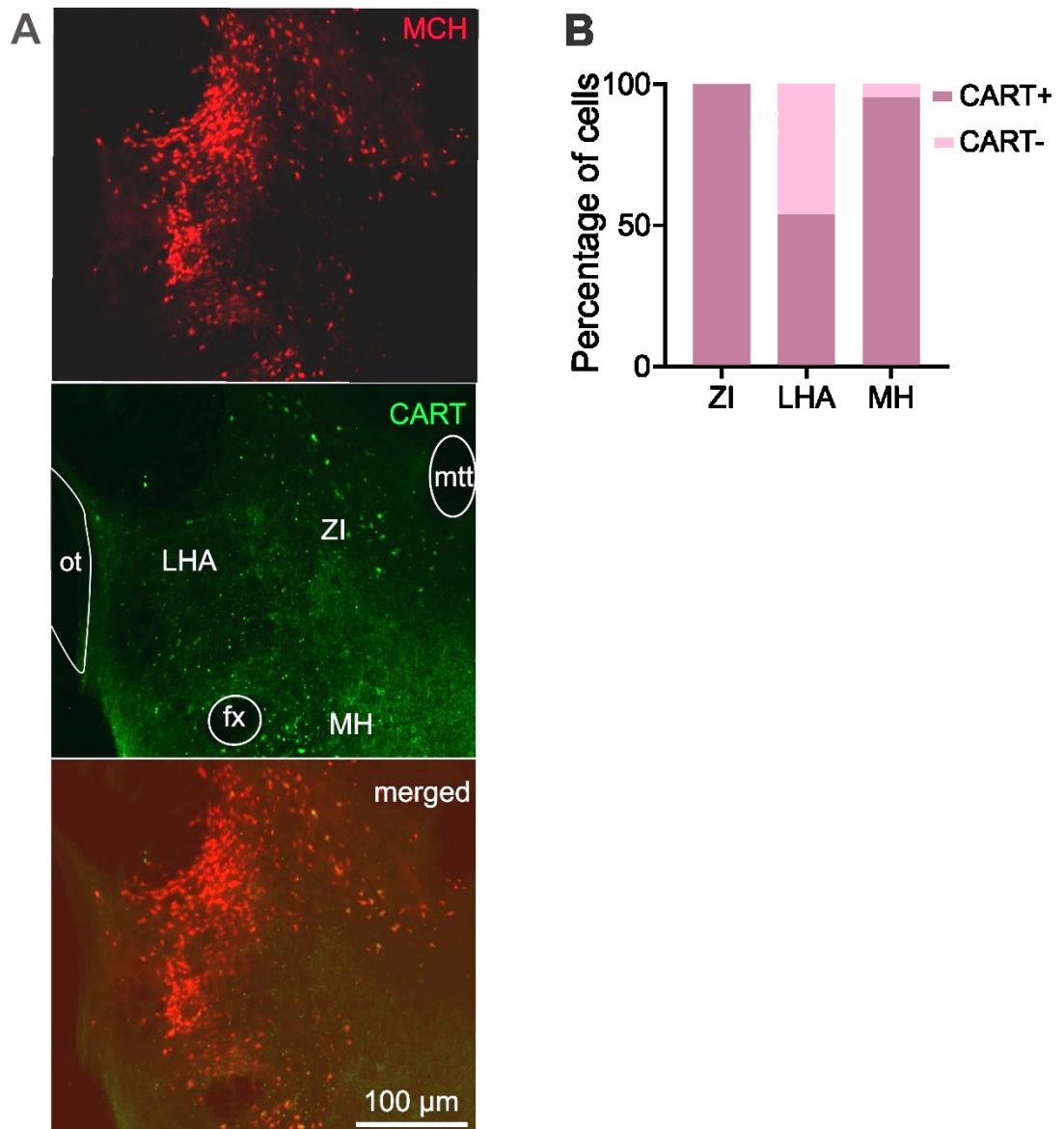


**Figure 20: Immunohistochemistry illustrating the distribution of MCH and CART neurons in the mouse hypothalamus.**

(A) Distribution of MCH+ (red, top panel) and CART+ (green, middle panel) neurons in three hypothalamic regions indicated by: Zona incerta (ZI), lateral hypothalamic area (LHA) and medial hypothalamus (MH). Merged illustration of MCH and CART immunohistochemistry (bottom panel) delineating the expression of MCH and CART neurons particularly MCH+/CART- neurons in the LHA. (See Figure 13 for close-up images of CART-immunopositive and negative MCH neurons).

(B) Proportion of CART-expressing and CART non-expressing MCH neurons that fired action potentials in the three areas.

fx: fornix, mtt: medullomamillary tract, ot: optic tract

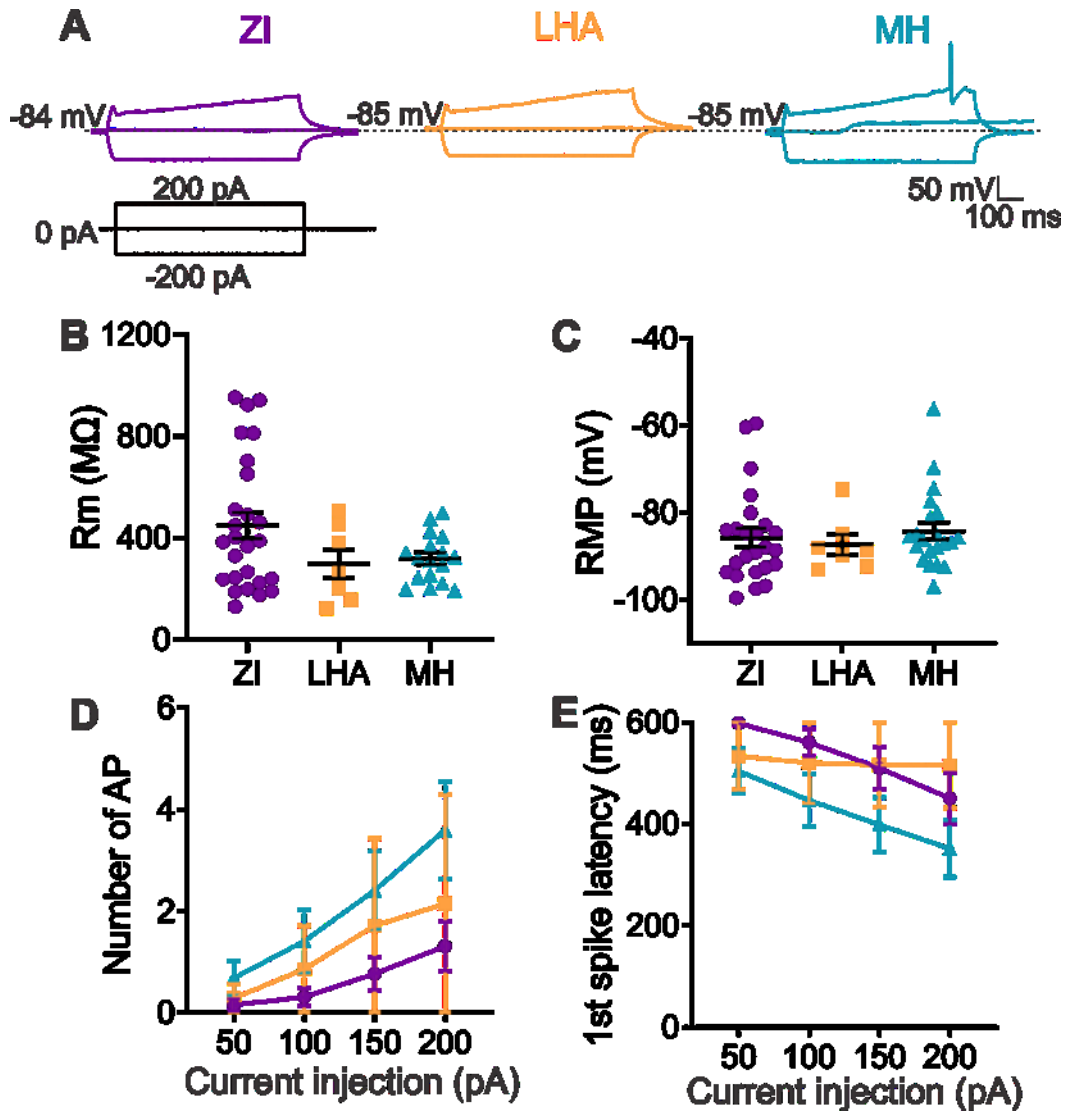


**Figure 21: Excitability of MCH+*CART*+ neurons in distinct hypothalamic areas**  
 (A) Representative current clamp recordings from MCH neurons from MCH+/*CART*+ neurons from three hypothalamic areas.  
 (B) Membrane resistance ( $R_m$ ) of MCH neurons.  
 (C) Resting membrane potential of MCH neurons.  
 (D-E) Number of action potentials (AP) (D) and latency to first spike (E) in response to various current injections. *Mean  $\pm$  SEM.*

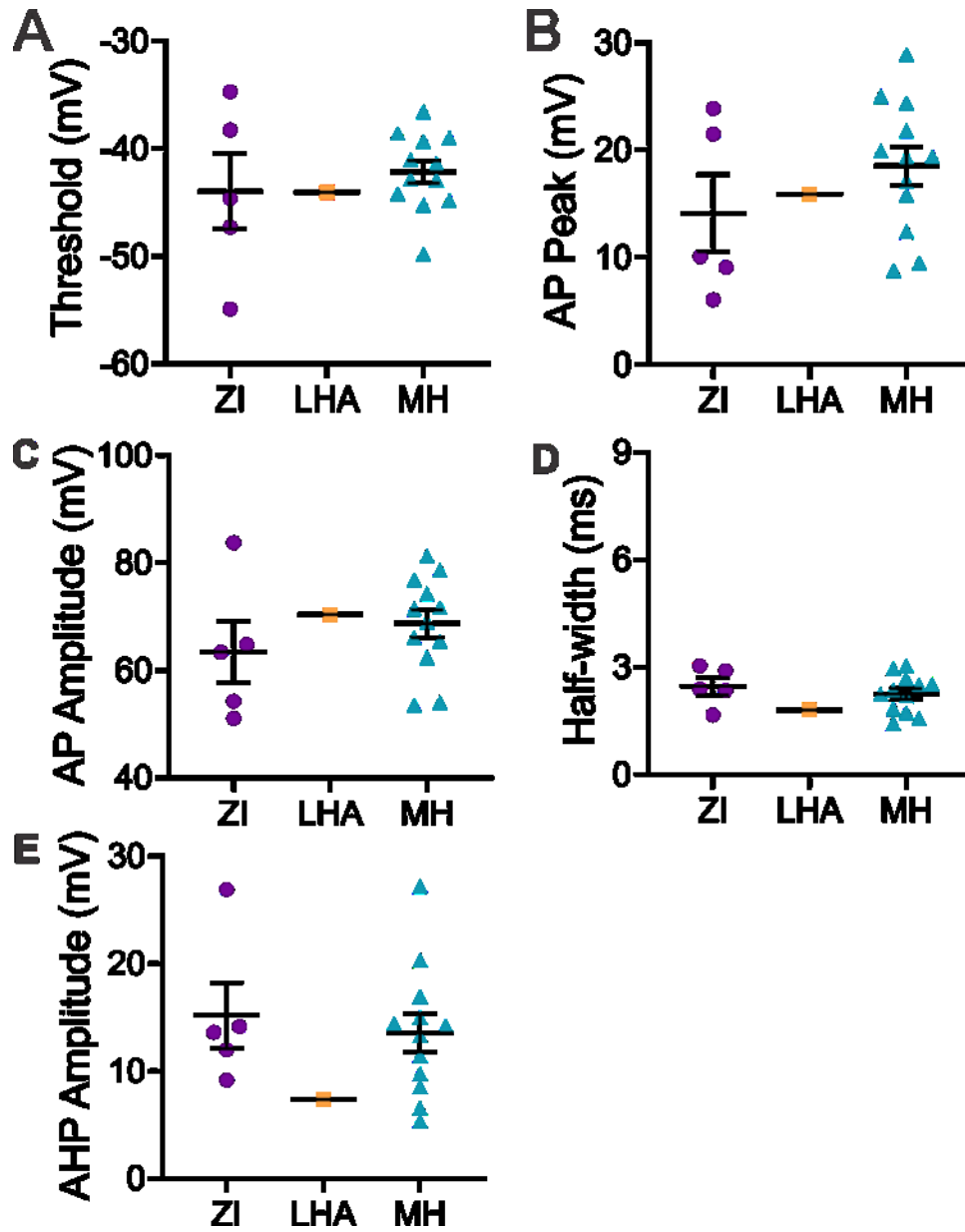


Figure 22: Anatomical area differences among MCH+/CART+ neurons.

(A-E). Various parameters of AP waveform including Threshold (A), Action potential (AP) peak (B), AP amplitude (C), after-hyperpolarization (AHP, D), and half-width (E) of MCH+/CART+ neurons. *Mean  $\pm$  SEM.*

## CHAPTER 4

### DISCUSSION

#### 4.1 Anatomical Subpopulations of MCH Neurons

This study provides evidence MCH neurons exist as spatially distinct subpopulations that are distributed in the hypothalamus. Our results show that LHA MCH neurons are more excitable than ZI or MH MCH neurons. This excitability is characterized by LHA MCH neurons being more sensitive to depolarizing current injections; as current injection intensified, these LHA neurons discharged more AP with shorter latency to first spike. MH MCH neurons also fired higher number of AP with current injection but required higher current injection (rheobase 150-200pA) compared to LHA neurons, which required less (100pA). In contrast, ZI MCH neurons required the highest current injection to evoke an AP, often firing just one or a few APs with maximum current injection. In fact, the greater excitability displayed by LHA MCH neurons was consistent when cells were held at subthreshold potential to ensure they all fire AP. Excitability of neurons is regulated by ion channels like voltage gated sodium and potassium channels (du Lac, 1996).

Sodium channels open with membrane depolarization and facilitate the inward current of sodium ions that allows the upward stroke of action potential in nerve cells (de Lera Ruiz & Kraus, 2015; Z. Li et al., 2021). Delayed rectifiers are voltage-gated potassium channels that are activated by depolarized membrane potential and act to

repolarize the neurons during action potentials via potassium efflux (Kim & Nimigean, 2016). Another type of potassium channels is the inwardly rectifying potassium channels. These potassium channels conduct potassium with hyperpolarized potential in contrast to depolarization in other types of potassium channels (Kuang et al., 2015). Conductance of these ion channels may underlie cellular changes that occur with states such as sleep, hunger, or novel object exploration (Nelson et al., 2003). Therefore, it is likely that excitability of MCH neurons is context dependent. Indeed, in-vivo experiments have shown that LHA MCH neurons are silent during waking, minimally active during NREM sleep and maximally active during REM sleep (Jones & Hassani, 2013). Supporting this is evidence that there is upregulation of MCH in hypothalamic MCH neurons during the sleep cycle in rats (Blanco-Centurion et al., 2019; Harthoorn et al., 2005).

Three functionally distinct subpopulations of LHA MCH neurons have been described: those that are only active during wakefulness, REM sleep active MCH neurons and those that are active during both wakefulness and REM sleep (Izawa et al., 2019). Moreover, optical recordings from LHA specific MCH neurons showed that MCH neurons display increased activity during novel object but not familiar object exploration (Blanco-Centurion et al., 2019; González et al., 2016). MCH neurons also play a role in food intake and seeking behaviours, thus wake active MCH neurons might be involved in these behaviours as well. However, it should be noted that most of these experiments have been *in vivo* while our experiments have been *in vitro*. Therefore, we cannot

conclude that cellular changes that occur due to physiological stimuli or behaviours prior to experiments remain during *in vitro* recordings.

Since membrane properties are shaped by ionic conductance, it is likely that the differences in excitability observed in anatomical subpopulations of MCH neurons are mediated by variations in the expression and activity of ion channels. MCH neurons also receive considerable inputs from across the brain, which could influence their excitability. Some of these inputs are mediated by interneurons (such as glutamatergic and GABAergic interneurons and ion channels (Diniz & Bittencourt, 2017; Gao & van den Pol, 2001). Activation of metabotropic glutamate receptors (mGluR) excites MCH neurons, causing membrane depolarization and increase in spike frequency (Huang & van den Pol, 2007). In support of this, rodents lacking mGluR subtype 5 (mGluR5) weighed less than their wildtype littermates, even when food intake was similar (Bradbury et al., 2005). Also, after food deprivation, rodents with their mGluR5 knocked out had decreased re-feeding rate compared to mGluR5 wildtype rodents. Comparably, an mGluR5 antagonist led to decreased re-feeding after fasting in mGluR5 wildtype rodents compared to mGluR5 knockout mice suggesting that suppression of feeding may be mediated by mGluR5 activation (Bradbury et al., 2005).

Furthermore, MCH neurons in the LHA have been shown to receive inputs from the orexigenic neuropeptide Y (NPY) neurons (Van Den Pol et al., 2004). NPY inhibits MCH neurons, hyperpolarizing the membrane potential and reducing firing frequency through the G-protein gated inwardly rectifying potassium (GIRK) currents (Van Den Pol

et al., 2004). Reports have shown that MCH neurons are activated by orexin neurons where orexin increases glutamatergic inputs to MCH neurons (Van Den Pol et al., 2004). However, another study showed that orexin has a dual effect on MCH neurons where optogenetic activation of orexin neurons in LHA slices activated some MCH neurons while inhibiting others by increasing GABA inputs to MCH neurons (Apergis-Schoute et al., 2015). Taking all these together, it is possible that differences in excitability seen in anatomical subpopulations of MCH neurons is due to varied inputs to these brain areas affecting the ion channel signalling and ultimately the membrane properties.

MCH neurons are located most prominently in the LHA and many studies focus on the LHA MCH neurons only and disregard the MH and ZI, even though MCH neurons are located extensively in these areas as well. As a result, details about the characteristics and functions of MH and ZI MCH neurons are scarce. Our study has shown that these neurons may not be functionally the same and there may be diversity among neurons in the same area. Consequently, the anatomical subpopulations of MCH neurons, their inputs and projections need to be investigated further.

## **4.2 Neurochemical Subpopulations of MCH Neurons**

The present study corroborates previous studies that CART is co-expressed by MCH neurons and that these cells occupy distinct areas of the hypothalamus. Within the hypothalamic regions where MCH neurons are localized, MCH+/CART+ neurons were observed widely within the ZI, LHA and MH, while MCH+/CART- neurons were found

almost exclusively in the LHA with sparse neurons in the ZI and MH. These results are consistent with previous similar studies (Croizier et al., 2010; Cvetkovic et al., 2004) where most of the MCH+/CART+ neurons were observed throughout the MCH-containing area including the ZI and regions medial to the fornix (i.e., MH) with very few MCH+/CART- neurons in these areas. MCH+/CART- neurons in contrast were observed to be mainly in the LHA including the perifornical area (Cvetkovic et al., 2004).

The main results obtained in this study demonstrates that CART is co-expressed in a subset of MCH neurons, and that these cells have different electrophysiological properties to MCH+/CART- neurons. The general electrophysiological properties of MCH neurons have been described in previous studies. MCH neurons are relatively hyperpolarized, spontaneously silent at rest, express A-type current and spike adaptation with positive current injection and lack H-current (Belanger-Willoughby et al., 2016; Eggermann et al., 2003; van den Pol et al., 2004). In our study, MCH+/CART+ neurons displayed the characteristic MCH electrophysiological properties previously described: hyperpolarized and no H-current. These neurons have A-current, which delays the first spike, and reduces firing rate and excitability (Fransén & Tigerholm, 2009).

On the other hand, MCH+/CART- neurons are relatively depolarized at rest and display an H-current. The higher number of AP firing and shorter latency to first spike seen in MCH+/CART- neurons was most likely caused by depolarized RMP and the presence of H-current. Indeed, activation of H-current is known to lead to membrane

depolarization and increased excitability (Angelo & Margrie, 2011; Buskila et al., 2019; Lüthi & McCormick, 1998). Furthermore, the higher number of spikes in MCH+/CART- neurons may be contributed by the presence of the H-current; since H-current conductance promotes faster recovery from afterhyperpolarization, increasing the possibility for recurring firing (Dudman & Nolan, 2009).

MCH neurons project extensively throughout the CNS, which suggests that MCH neurons may function as a neuromodulator to regulate many physiological roles including food intake, sleep, and mood. While our work is the first to identify the presence of H-current in a subpopulation of MCH neurons, the expression and role of H-current in other neurons have been well documented. H-current has been proposed to control conduction velocity of axons, mainly by depolarizing the resting membrane potential (Byczkowicz et al., 2019; Debanne et al., 2011). H-current is conducted through the hyperpolarization-activated cyclic nucleotide gated (HCN) channels. These HCN channels are regulated by the second messenger cyclic AMP (cAMP). cAMP bind to and stimulates the HCN channels to open, leading to increased H-current (Wang et al., 2002). A previous study showed that neuromodulators like adenosine, which also act via cAMP-dependent pathway resulted in decreased conduction velocity while norepinephrine resulted in an increased conduction velocity via modulation of H-current (Byczkowicz et al., 2019). Like MCH, adenosine has been established as an endogenous sleep factor, mediating the sleep after prolonged wakefulness (Basheer et al., 2004; Porkka-Heiskanen et al., 1997). Therefore, it is possible that the cAMP-HCN pathway

modulating the H-current allows an increase in excitability of a subpopulation of MCH neurons during arousal but a decrease in their excitability during periods of rest or sleep to save metabolic cost.

As previously mentioned, neurochemical subpopulations of MCH neurons are found in different parts of the hypothalamus with MCH+/CART- neurons found majorly in the LHA and very few elsewhere (Figure 20B). As a result, area differences for each neurochemical subpopulation could not be performed in MCH+/CART- neurons.

However, area differences in excitability of MCH+/CART+ neurons were performed as they were found in all areas of the hypothalamus. These neurons showed no differences in excitability, which could mean that they contain the same proportion of ion channels, are excited by the same stimulus and possibly perform the same functions, independent of localization. Indeed, MCH+/CART+ neurons project to the hippocampus and septum while MCH+/CART- neurons send descending projections to the brainstem and spinal cord (Hanriot et al., 2007) supporting the notion that these subgroups are functionally different.

#### **4.3 Limitations of the study**

Our study shows evidence that anatomical and neurochemical subpopulations of MCH neurons exist. However, there are some limitations to our study including the sample size. For instance, to fully elucidate the electrophysiological differences between MCH+/CART+ and MCH+/CART- neurons, we need to increase the sample size for non-

CART expressing MCH neurons. Similarly, our study had fewer female mice, which limited our ability to elucidate any sex-dependent differences in both MCH neuron subpopulations. Furthermore, it will be of utmost importance to characterize any anatomical differences displayed by MCH+/CART- neurons in the LHA, ZI and MH. It should also be noted that our brain slices were collected during the light phase, and the time of the day may affect the electrophysiological properties of MCH neurons. Similarly, it is possible that these neuronal excitabilities may be plastic under different physiological states. That is, it remains to be seen whether the difference in excitability of MCH neurons change with different stimuli like sleep deprivation, diet, and memory experiments.

#### **4.4 Conclusion**

The current study has shown that anatomical subpopulation of MCH neurons exist. Particularly, LHA MCH neurons are more excitable than ZI and MH MCH neurons. In addition, we have also shown that neurochemical subpopulation of MCH neurons have different excitability: MCH+/CART- neurons are more excitable than MCH+/CART+ neurons. Notably, MCH+/CART- neurons were more abundant in the LHA. Therefore, it is possible that the higher excitability of LHA MCH neurons was due to the depolarized potential of MCH+/CART- neurons.

In conclusion, to our knowledge, this is the first study to compare the electrophysiological properties of MCH neuron subpopulations and to identify the presence of H-current in a distinct MCH subpopulation. The present investigation highlights the importance of ionic mechanisms underlying distinct characteristics of these cell subpopulations. Therefore, to understand the mechanism of action of the MCH system in its diverse physiological functions, further characterization of these subpopulations must be performed. This will be a step towards identification of functional subpopulations of MCH neurons.

## REFERENCES

- Abbott, C. R., Kennedy, A. R., Wren, A. M., Rossi, M., Murphy, K. G., Seal, L. J., Todd, J. F., Ghatei, M. A., Small, C. J., & Bloom, S. R. (2003). Identification of Hypothalamic Nuclei Involved in the Orexigenic Effect of Melanin-Concentrating Hormone. *Endocrinology*, *144*(9), 3943–3949. <https://doi.org/10.1210/en.2003-0149>
- Adamantidis, A., & de Lecea, L. (2009). A role for Melanin-Concentrating Hormone in learning and memory. *Peptides*, *30*(11), 2066–2070. <https://doi.org/10.1016/j.peptides.2009.06.024>
- Adamantidis, A., Salvert, D., Goutagny, R., Lakaye, B., Gervasoni, D., Grisar, T., Luppi, P. H., & Fort, P. (2008). Sleep architecture of the melanin-concentrating hormone receptor 1-knockout mice. *European Journal of Neuroscience*. <https://doi.org/10.1111/j.1460-9568.2008.06129.x>
- Adell, A., Celada, P., Abellán, M. T., & Artigas, F. (2002). Origin and functional role of the extracellular serotonin in the midbrain raphe nuclei. *Brain Research Reviews*, *39*(2–3), 154–180. [https://doi.org/10.1016/S0165-0173\(02\)00182-0](https://doi.org/10.1016/S0165-0173(02)00182-0)
- Ahnaou, A., Drinkenburg, W. H. I. M., Bouwknecht, J. A., Alcazar, J., Steckler, T., & Dautzenberg, F. M. (2008). Blocking melanin-concentrating hormone MCH1 receptor affects rat sleep-wake architecture. *European Journal of Pharmacology*, *579*(1–3), 177–188. <https://doi.org/10.1016/j.ejphar.2007.10.017>
- Aja, S., Sahandy, S., Ladenheim, E. E., Schwartz, G. J., & Moran, T. H. (2001). Intracerebroventricular CART peptide reduces food intake and alters motor behavior at a hindbrain site. *American Journal of Physiology-Regulatory, Integrative and Comparative Physiology*, *281*(6), R1862–R1867. <https://doi.org/10.1152/ajpregu.2001.281.6.R1862>
- Angelo, K., & Margrie, T. W. (2011). Population diversity and function of hyperpolarization-activated current in olfactory bulb mitral cells. *Scientific Reports*, *1*(1), 50. <https://doi.org/10.1038/srep00050>
- Apergis-Schoute, J., Iordanidou, P., Faure, C., Jegu, S., Schöne, C., Aitta-Aho, T., Adamantidis, A., & Burdakov, D. (2015). Optogenetic Evidence for Inhibitory Signaling from Orexin to MCH Neurons via Local Microcircuits. *The Journal of Neuroscience*, *35*(14), 5435–5441. <https://doi.org/10.1523/JNEUROSCI.5269-14.2015>
- Bächner, D., Kreienkamp, H.-J., Weise, C., Buck, F., & Richter, D. (1999). Identification of melanin concentrating hormone (MCH) as the natural ligand for the orphan somatostatin-like receptor 1 (SLC-1). *FEBS Letters*, *457*(3), 522–524. [https://doi.org/10.1016/S0014-5793\(99\)01092-3](https://doi.org/10.1016/S0014-5793(99)01092-3)
- Basheer, R., Strecker, R. E., Thakkar, M. M., & McCarley, R. W. (2004). Adenosine and sleep–wake regulation. *Progress in Neurobiology*, *73*(6), 379–396. <https://doi.org/10.1016/j.pneurobio.2004.06.004>

- Belanger-Willoughby, N., Linehan, V., & Hirasawa, M. (2016). Thermosensing mechanisms and their impairment by high-fat diet in orexin neurons. *Neuroscience*, 324, 82–91. <https://doi.org/10.1016/j.neuroscience.2016.03.003>
- Bellinger, L. L., & Bernardis, L. L. (2002). The dorsomedial hypothalamic nucleus and its role in ingestive behavior and body weight regulation. *Physiology & Behavior*, 76(3), 431–442. [https://doi.org/10.1016/S0031-9384\(02\)00756-4](https://doi.org/10.1016/S0031-9384(02)00756-4)
- Bittencourt, J. C., & Elias, C. F. (1998). Melanin-concentrating hormone and neuropeptide EI projections from the lateral hypothalamic area and zona incerta to the medial septal nucleus and spinal cord: A study using multiple neuronal tracers. *Brain Research*, 805(1–2), 1–19. [https://doi.org/10.1016/S0006-8993\(98\)00598-8](https://doi.org/10.1016/S0006-8993(98)00598-8)
- Bittencourt, J. C., Presse, F., Arias, C., Peto, C., Vaughan, J., Nahon, J. -L, Vale, W., & Sawchenko, P. E. (1992). The melanin-concentrating hormone system of the rat brain: An immuno- and hybridization histochemical characterization. *Journal of Comparative Neurology*, 319(2), 218–245. <https://doi.org/10.1002/cne.903190204>
- Blanco-Centurion, C., Liu, M., Konadhode, R. P., Zhang, X., Pelluru, D., van den Pol, A. N., & Shiromani, P. J. (2016). Optogenetic activation of melanin-concentrating hormone neurons increases non-rapid eye movement and rapid eye movement sleep during the night in rats. *European Journal of Neuroscience*. <https://doi.org/10.1111/ejn.13410>
- Blanco-Centurion, C., Luo, S., Spergel, D. J., Vidal-Ortiz, A., Oprisan, S. A., Van den Pol, A. N., Liu, M., & Shiromani, P. J. (2019). Dynamic Network Activation of Hypothalamic MCH Neurons in REM Sleep and Exploratory Behavior. *The Journal of Neuroscience : The Official Journal of the Society for Neuroscience*, 39(25), 4986–4998. <https://doi.org/10.1523/JNEUROSCI.0305-19.2019>
- Borowsky, B., Durkin, M. M., Ogozalek, K., Marzabadi, M. R., DeLeon, J., Heurich, R., Lichtblau, H., Shaposhnik, Z., Daniewska, I., Blackburn, T. P., Branchek, T. A., Gerald, C., Vaysse, P. J., & Forray, C. (2002). Antidepressant, anxiolytic and anorectic effects of a melanin-concentrating hormone-1 receptor antagonist. *Nature Medicine*, 8(8), 825–830. <https://doi.org/10.1038/nm741>
- Bradbury, M. J., Campbell, U., Giracello, D., Chapman, D., King, C., Tehrani, L., Cosford, N. D. P., Anderson, J., Varney, M. A., & Strack, A. M. (2005). Metabotropic Glutamate Receptor mGlu5 Is a Mediator of Appetite and Energy Balance in Rats and Mice. *Journal of Pharmacology and Experimental Therapeutics*, 313(1), 395–402. <https://doi.org/10.1124/jpet.104.076406>
- Burdakov, D., Gerasimenko, O., & Verkhratsky, A. (2005). Physiological Changes in Glucose Differentially Modulate the Excitability of Hypothalamic Melanin-Concentrating Hormone and Orexin Neurons *In Situ*. *The Journal of Neuroscience*, 25(9), 2429–2433. <https://doi.org/10.1523/JNEUROSCI.4925-04.2005>
- Buskila, Y., Kékesi, O., Bellot-Saez, A., Seah, W., Berg, T., Trpceski, M., Yerbury, J. J., & Ooi, L. (2019). Dynamic interplay between H-current and M-current controls motoneuron hyperexcitability in amyotrophic lateral sclerosis. *Cell Death & Disease*, 10(4), 310. <https://doi.org/10.1038/s41419-019-1538-9>

- Byczkowicz, N., Eshra, A., Montanaro, J., Trevisiol, A., Hirrlinger, J., Kole, M. H., Shigemoto, R., & Hallermann, S. (2019). HCN channel-mediated neuromodulation can control action potential velocity and fidelity in central axons. *ELife*, 8. <https://doi.org/10.7554/eLife.42766>
- Chambers, J., Ames, R. S., Bergsma, D., Muir, A., Fitzgerald, L. R., Hervieu, G., Dytko, G. M., Foley, J. J., Martin, J., Liu, W. S., Park, J., Ellis, C., Ganguly, S., Konchar, S., Cluderay, J., Leslie, R., Wilson, S., & Sarau, H. M. (1999). Melanin-concentrating hormone is the cognate ligand for the orphan G- protein-coupled receptor SLC-1. *Nature*. <https://doi.org/10.1038/22313>
- Chee, M. J. S., Pissios, P., & Maratos-Flier, E. (2013). Neurochemical characterization of neurons expressing melanin-concentrating hormone receptor 1 in the mouse hypothalamus. *Journal of Comparative Neurology*. <https://doi.org/10.1002/cne.23273>
- Chen, Y., Hu, C., Hsu, C.-K., Zhang, Q., Bi, C., Asnicar, M., Hsiung, H. M., Fox, N., Sliker, L. J., Yang, D. D., Heiman, M. L., & Shi, Y. (2002). Targeted Disruption of the Melanin-Concentrating Hormone Receptor-1 Results in Hyperphagia and Resistance to Diet-Induced Obesity. *Endocrinology*, 143(7), 2469–2477. <https://doi.org/10.1210/endo.143.7.8903>
- Chou, T. C., Scammell, T. E., Gooley, J. J., Gaus, S. E., Saper, C. B., & Lu, J. (2003). Critical Role of Dorsomedial Hypothalamic Nucleus in a Wide Range of Behavioral Circadian Rhythms. *The Journal of Neuroscience*, 23(33), 10691–10702. <https://doi.org/10.1523/JNEUROSCI.23-33-10691.2003>
- Croizier, S., Franchi-Bernard, G., Colard, C., Poncet, F., La Roche, A., & Risold, P.-Y. (2010). A Comparative Analysis Shows Morphofunctional Differences between the Rat and Mouse Melanin-Concentrating Hormone Systems. *PLoS ONE*, 5(11), e15471. <https://doi.org/10.1371/journal.pone.0015471>
- Cvetkovic, V., Brischoux, F., Jacquemard, C., Fellmann, D., Griffond, B., & Risold, P. Y. (2004). Characterization of subpopulations of neurons producing melanin-concentrating hormone in the rat ventral diencephalon. *Journal of Neurochemistry*. <https://doi.org/10.1111/j.1471-4159.2004.02776.x>
- David, D. J., Klemenhagen, K. C., Holick, K. A., Saxe, M. D., Mendez, I., Santarelli, L., Craig, D. A., Zhong, H., Swanson, C. J., Hegde, L. G., Ping, X. I., Dong, D., Marzabadi, M. R., Gerald, C. P., & Hen, R. (2007). Efficacy of the MCHR1 antagonist N-[3-(1-{[4-(3,4-difluorophenoxy)phenyl]methyl}(4-piperidyl))-4-methylphenyl]-2-methylpropanamide (SNAP 94847) in mouse models of anxiety and depression following acute and chronic administration is independent of hippocampal neurogenesis. *The Journal of Pharmacology and Experimental Therapeutics*, 321(1), 237–248. <https://doi.org/10.1124/jpet.106.109678>
- de Lera Ruiz, M., & Kraus, R. L. (2015). Voltage-Gated Sodium Channels: Structure, Function, Pharmacology, and Clinical Indications. *Journal of Medicinal Chemistry*, 58(18), 7093–7118. <https://doi.org/10.1021/jm501981g>

- Debanne, D., Campanac, E., Bialowas, A., Carlier, E., & Alcaraz, G. (2011). Axon physiology. *Physiological Reviews*, *91*(2), 555–602. <https://doi.org/10.1152/physrev.00048.2009>
- Dimicco, J. A., & Zaretsky, D. V. (2007). The dorsomedial hypothalamus: a new player in thermoregulation. *American Journal of Physiology. Regulatory, Integrative and Comparative Physiology*, *292*(1), R47-63. <https://doi.org/10.1152/ajpregu.00498.2006>
- Diniz, G. B., & Bittencourt, J. C. (2017). The Melanin-Concentrating Hormone as an Integrative Peptide Driving Motivated Behaviors. *Frontiers in Systems Neuroscience*, *11*, 32. <https://doi.org/10.3389/fnsys.2017.00032>
- Douglass, J., McKinzie, A., & Couceyro, P. (1995). PCR differential display identifies a rat brain mRNA that is transcriptionally regulated by cocaine and amphetamine. *The Journal of Neuroscience*, *15*(3), 2471–2481. <https://doi.org/10.1523/JNEUROSCI.15-03-02471.1995>
- du Lac, S. (1996). Candidate cellular mechanisms of vestibulo-ocular reflex plasticity. *Annals of the New York Academy of Sciences*, *781*, 489–498. <https://doi.org/10.1111/j.1749-6632.1996.tb15722.x>
- Dudman, J. T., & Nolan, M. F. (2009). Stochastically Gating Ion Channels Enable Patterned Spike Firing through Activity-Dependent Modulation of Spike Probability. *PLoS Computational Biology*, *5*(2), e1000290. <https://doi.org/10.1371/journal.pcbi.1000290>
- Eggermann, E., Bayer, L., Serafin, M., Saint-Mleux, B., Bernheim, L., Machard, D., Jones, B. E., & Mühlethaler, M. (2003). The Wake-Promoting Hypocretin–Orexin Neurons Are in an Intrinsic State of Membrane Depolarization. *The Journal of Neuroscience*, *23*(5), 1557–1562. <https://doi.org/10.1523/JNEUROSCI.23-05-01557.2003>
- Elias, C. F., Sita, L. V., Zambon, B. K., Oliveira, E. R., Vasconcelos, L. A. P., & Bittencourt, J. C. (2008). Melanin-concentrating hormone projections to areas involved in somatomotor responses. *Journal of Chemical Neuroanatomy*, *35*(2), 188–201. <https://doi.org/10.1016/j.jchemneu.2007.10.002>
- Faber, C. L., Deem, J. D., Phan, B. A., Doan, T. P., Ogimoto, K., Mirzadeh, Z., Schwartz, M. W., & Morton, G. J. (2021). Leptin receptor neurons in the dorsomedial hypothalamus regulate diurnal patterns of feeding, locomotion, and metabolism. *eLife*, *10*. <https://doi.org/10.7554/eLife.63671>
- Fransén, E., & Tigerholm, J. (2009). Role of A-type potassium currents in excitability, network synchronicity, and epilepsy. *Hippocampus*, NA-NA. <https://doi.org/10.1002/hipo.20694>
- Gao, X., & Pol, A. N. (2001). Melanin concentrating hormone depresses synaptic activity of glutamate and GABA neurons from rat lateral hypothalamus. *The Journal of Physiology*, *533*(1), 237–252. <https://doi.org/10.1111/j.1469-7793.2001.0237b.x>
- Gautvik, K. M., de Lecea, L., Gautvik, V. T., Danielson, P. E., Tranque, P., Dopazo, A., Bloom, F. E., & Sutcliffe, J. G. (1996). Overview of the most prevalent hypothalamus-specific mRNAs, as identified by directional tag PCR subtraction.

- Proceedings of the National Academy of Sciences*, 93(16), 8733–8738.  
<https://doi.org/10.1073/pnas.93.16.8733>
- Georgescu, D., Sears, R. M., Hommel, J. D., Barrot, M., Bolaños, C. A., Marsh, D. J., Bednarek, M. A., Bibb, J. A., Maratos-Flier, E., Nestler, E. J., & DiLeone, R. J. (2005). The hypothalamic neuropeptide melanin-concentrating hormone acts in the nucleus accumbens to modulate feeding behavior and forced-swim performance. *Journal of Neuroscience*, 25(11), 2933–2940.  
<https://doi.org/10.1523/JNEUROSCI.1714-04.2005>
- Glick, M., Segal-Lieberman, G., Cohen, R., & Kronfeld-Schor, N. (2009). Chronic MCH infusion causes a decrease in energy expenditure and body temperature, and an increase in serum IGF-1 levels in mice. *Endocrine*. <https://doi.org/10.1007/s12020-009-9252-5>
- Gomori, A., Ishihara, A., Ito, M., Mashiko, S., Matsushita, H., Yumoto, M., Tanaka, T., Tokita, S., Moriya, M., Iwaasa, H., & Kanatani, A. (2003). Chronic intracerebroventricular infusion of MCH causes obesity in mice. Melanin-concentrating hormone. *Am J Physiol Endocrinol Metab*.
- González, J. A., Iordanidou, P., Strom, M., Adamantidis, A., & Burdakov, D. (2016). Awake dynamics and brain-wide direct inputs of hypothalamic MCH and orexin networks. *Nature Communications*, 7(1), 11395. <https://doi.org/10.1038/ncomms11395>
- Gooley, J. J., Schomer, A., & Saper, C. B. (2006). The dorsomedial hypothalamic nucleus is critical for the expression of food-entrainable circadian rhythms. *Nature Neuroscience*, 9(3), 398–407. <https://doi.org/10.1038/nn1651>
- Groessl, F., Jeong, J. H., Talmage, D. A., Role, L. W., & Jo, Y.-H. (2013). Overnight Fasting Regulates Inhibitory Tone to Cholinergic Neurons of the Dorsomedial Nucleus of the Hypothalamus. *PLoS ONE*, 8(4), e60828.  
<https://doi.org/10.1371/journal.pone.0060828>
- Haemmerle, C. A. S., Campos, A. M. P., & Bittencourt, J. C. (2015). Melanin-concentrating hormone inputs to the nucleus accumbens originate from distinct hypothalamic sources and are apposed to GABAergic and cholinergic cells in the Long-Evans rat brain. *Neuroscience*, 289, 392–405.  
<https://doi.org/10.1016/j.neuroscience.2015.01.014>
- Hanriot, L., Camargo, N., Courau, A. C., Leger, L., Luppi, P. H., & Peyron, C. (2007). Characterization of the melanin-concentrating hormone neurons activated during paradoxical sleep hypersomnia in rats. *Journal of Comparative Neurology*.  
<https://doi.org/10.1002/cne.21482>
- Harthoorn, L. F., Sañé, A., Nethe, M., & Van Heerikhuize, J. J. (2005). Multi-transcriptional profiling of melanin-concentrating hormone and orexin-containing neurons. *Cellular and Molecular Neurobiology*, 25(8), 1209–1223.  
<https://doi.org/10.1007/s10571-005-8184-8>
- Hassani, O. K., Lee, M. G., & Jones, B. E. (2009). Melanin-concentrating hormone neurons discharge in a reciprocal manner to orexin neurons across the sleep-wake

- cycle. *Proceedings of the National Academy of Sciences of the United States of America*. <https://doi.org/10.1073/pnas.0811400106>
- Hausen, A. C., Ruud, J., Jiang, H., Hess, S., Varbanov, H., Kloppenburg, P., & Brüning, J. C. (2016). Insulin-Dependent Activation of MCH Neurons Impairs Locomotor Activity and Insulin Sensitivity in Obesity. *Cell Reports*. <https://doi.org/10.1016/j.celrep.2016.11.030>
- Huang, H., & van den Pol, A. N. (2007). Rapid Direct Excitation and Long-Lasting Enhancement of NMDA Response by Group I Metabotropic Glutamate Receptor Activation of Hypothalamic Melanin-Concentrating Hormone Neurons. *The Journal of Neuroscience*, 27(43), 11560–11572. <https://doi.org/10.1523/JNEUROSCI.2147-07.2007>
- Izawa, S., Chowdhury, S., Miyazaki, T., Mukai, Y., Ono, D., Inoue, R., Ohmura, Y., Mizoguchi, H., Kimura, K., Yoshioka, M., Terao, A., Kilduff, T. S., & Yamanaka, A. (2019). REM sleep–active MCH neurons are involved in forgetting hippocampus-dependent memories. *Science*, 365(6459), 1308–1313. <https://doi.org/10.1126/science.aax9238>
- Jego, S., Glasgow, S. D., Herrera, C. G., Ekstrand, M., Reed, S. J., Boyce, R., Friedman, J., Burdakov, D., & Adamantidis, A. R. (2013). Optogenetic identification of a rapid eye movement sleep modulatory circuit in the hypothalamus. *Nature Neuroscience*, 16(11), 1637–1643. <https://doi.org/10.1038/nn.3522>
- Jeon, J. Y., Bradley, R. L., Kokkotou, E. G., Marino, F. E., Wang, X., Pissios, P., & Maratos-Flier, E. (2006). MCH-/- mice are resistant to aging-associated increases in body weight and insulin resistance. *Diabetes*, 55(2), 428–434. <https://doi.org/10.2337/diabetes.55.02.06.db05-0203>
- Jeong, J. H., Lee, D. K., & Jo, Y.-H. (2017). Cholinergic neurons in the dorsomedial hypothalamus regulate food intake. *Molecular Metabolism*, 6(3), 306–312. <https://doi.org/10.1016/j.molmet.2017.01.001>
- Jones, B. E., & Hassani, O. K. (2013). The Role of Hcrt/Orx and MCH Neurons in Sleep-Wake State Regulation. *Sleep*, 36(12), 1769–1772. <https://doi.org/10.5665/sleep.3188>
- Kawauchi, H., Kawazoe, I., Tsubokawa, M., Kishida, M., & Baker, B. I. (1983). Characterization of melanin-concentrating hormone in chum salmon pituitaries. *Nature*. <https://doi.org/10.1038/305321a0>
- Kim, D. M., & Nimigeon, C. M. (2016). Voltage-Gated Potassium Channels: A Structural Examination of Selectivity and Gating. *Cold Spring Harbor Perspectives in Biology*, 8(5). <https://doi.org/10.1101/cshperspect.a029231>
- Kokkotou, E. G., Tritos, N. A., Mastaitis, J. W., Sliker, L., & Maratos-Flier, E. (2001). Melanin-Concentrating Hormone Receptor Is a Target of Leptin Action in the Mouse Brain. *Endocrinology*, 142(2), 680–686. <https://doi.org/10.1210/endo.142.2.7981>
- Kokkotou, E., Jeon, J. Y., Wang, X., Marino, F. E., Carlson, M., Trombly, D. J., & Maratos-Flier, E. (2005). Mice with MCH ablation resist diet-induced obesity through strain-

- specific mechanisms. *American Journal of Physiology - Regulatory Integrative and Comparative Physiology*. <https://doi.org/10.1152/ajpregu.00861.2004>
- Konadhode, R. R., Pelluru, D., Blanco-Centurion, C., Zayachkivsky, A., Liu, M., Uhde, T., Glen, W. B., van den Pol, A. N., Mulholland, P. J., & Shiromani, P. J. (2013). Optogenetic stimulation of MCH neurons increases sleep. *Journal of Neuroscience*, *33*(25), 10257–10263. <https://doi.org/10.1523/JNEUROSCI.1225-13.2013>
- Konadhode, R. R., Pelluru, D., & Shiromani, P. J. (2014). Neurons containing orexin or melanin concentrating hormone reciprocally regulate wake and sleep. *Frontiers in Systems Neuroscience*, *8*, 244. <https://doi.org/10.3389/fnsys.2014.00244>
- Kong, D., Vong, L., Parton, L. E., Ye, C., Tong, Q., Hu, X., Choi, B., Brüning, J. C., & Lowell, B. B. (2010). Glucose stimulation of hypothalamic MCH neurons involves K(ATP) channels, is modulated by UCP2, and regulates peripheral glucose homeostasis. *Cell Metabolism*, *12*(5), 545–552. <https://doi.org/10.1016/j.cmet.2010.09.013>
- Kosse, C., Gonzalez, A., & Burdakov, D. (2015). Predictive models of glucose control: roles for glucose-sensing neurones. *Acta Physiologica*, *213*(1), 7–18. <https://doi.org/10.1111/apha.12360>
- Koylu, E. O., Couceyro, P. R., Lambert, P. D., Ling, N. C., DeSouza, E. B., & Kuhar, M. J. (1997). Immunohistochemical Localization of Novel CART Peptides in Rat Hypothalamus, Pituitary and Adrenal Gland. *Journal of Neuroendocrinology*, *9*(11), 823–833. <https://doi.org/10.1046/j.1365-2826.1997.00651.x>
- Kuang, Q., Purhonen, P., & Hebert, H. (2015). Structure of potassium channels. *Cellular and Molecular Life Sciences : CMLS*, *72*(19), 3677–3693. <https://doi.org/10.1007/s00018-015-1948-5>
- Lagos, P., Urbanavicius, J., Scorza, M. C., Miraballes, R., & Torterolo, P. (2011). Depressive-like profile induced by MCH microinjections into the dorsal raphe nucleus evaluated in the forced swim test. *Behavioural Brain Research*, *218*(2), 259–266. <https://doi.org/10.1016/j.bbr.2010.10.035>
- Lambert, P. D., Couceyro, P. R., McGirr, K. M., Dall Vechia, S. E., Smith, Y., & Kuhar, M. J. (1998). CART peptides in the central control of feeding and interactions with neuropeptide Y. *Synapse (New York, N.Y.)*, *29*(4), 293–298. [https://doi.org/10.1002/\(SICI\)1098-2396\(199808\)29:4<293::AID-SYN1>3.0.CO;2-0](https://doi.org/10.1002/(SICI)1098-2396(199808)29:4<293::AID-SYN1>3.0.CO;2-0)
- Le Barillier, L., Léger, L., Luppi, P.-H., Fort, P., Malleret, G., & Salin, P.-A. (2015). Genetic deletion of melanin-concentrating hormone neurons impairs hippocampal short-term synaptic plasticity and hippocampal-dependent forms of short-term memory. *Hippocampus*, *25*(11), 1361–1373. <https://doi.org/10.1002/hipo.22442>
- Limbo, P. M. C., Grazzini, E., Cao, J., Hubatsch, D. A., Pelletier, M., Hoffert, C., St-Onge, S., Pou, C., Labrecque, J., Groblewski, T., O'Donnell, D., Payza, K., Ahmad, S., & Walker, P. (1999). The receptor for the orexigenic peptide melanin-concentrating hormone is a G-protein-coupled receptor. *Nature Cell Biology*. <https://doi.org/10.1038/12978>
- Li, L., Zhang, M.-Q., Sun, X., Liu, W.-Y., Huang, Z.-L., & Wang, Y.-Q. (2022). Role of Dorsomedial Hypothalamus GABAergic Neurons in Sleep–Wake States in Response

- to Changes in Ambient Temperature in Mice. *International Journal of Molecular Sciences*, 23(3), 1270. <https://doi.org/10.3390/ijms23031270>
- Li, Z., Rizzi, G., & Tan, K. R. (2021). Zona incerta subpopulations differentially encode and modulate anxiety. *Science Advances*, 7(37). <https://doi.org/10.1126/sciadv.abf6709>
- Lima, F. F. B., Sita, L. V., Oliveira, A. R., Costa, H. C., da Silva, J. M., Mortara, R. A., Haemmerle, C. A. S., Xavier, G. F., Canteras, N. S., & Bittencourt, J. C. (2013). Hypothalamic melanin-concentrating hormone projections to the septo-hippocampal complex in the rat. *Journal of Chemical Neuroanatomy*, 47, 1–14. <https://doi.org/10.1016/j.jchemneu.2012.10.003>
- Linehan, V., & Hirasawa, M. (2018). Electrophysiological Properties of Melanin-Concentrating Hormone and Orexin Neurons in Adolescent Rats. *Frontiers in Cellular Neuroscience*, 12. <https://doi.org/10.3389/fncel.2018.00070>
- Liu, K., Kim, J., Kim, D. W., Zhang, Y. S., Bao, H., Denaxa, M., Lim, S.-A., Kim, E., Liu, C., Wickersham, I. R., Pachnis, V., Hattar, S., Song, J., Brown, S. P., & Blackshaw, S. (2017). Lhx6-positive GABA-releasing neurons of the zona incerta promote sleep. *Nature*, 548(7669), 582–587. <https://doi.org/10.1038/nature23663>
- López Hill, X., Pascovich, C., Urbanavicius, J., Torterolo, P., & Scorza, M. C. (2013). The median raphe nucleus participates in the depressive-like behavior induced by MCH: differences with the dorsal raphe nucleus. *Peptides*, 50, 96–99. <https://doi.org/10.1016/j.peptides.2013.10.002>
- Lu, J., Greco, M. A., Shiromani, P., & Saper, C. B. (2000). Effect of lesions of the ventrolateral preoptic nucleus on NREM and REM sleep. *The Journal of Neuroscience : The Official Journal of the Society for Neuroscience*, 20(10), 3830–3842. <https://doi.org/10.1523/JNEUROSCI.20-10-03830.2000>
- Ludwig, D. S., Tritos, N. A., Mastaitis, J. W., Kulkarni, R., Kokkotou, E., Elmquist, J., Lowell, B., Flier, J. S., & Maratos-Flier, E. (2001). Melanin-concentrating hormone overexpression in transgenic mice leads to obesity and insulin resistance. *Journal of Clinical Investigation*. <https://doi.org/10.1172/JCI10660>
- Lüthi, A., & McCormick, D. A. (1998). H-current: properties of a neuronal and network pacemaker. *Neuron*, 21(1), 9–12. [https://doi.org/10.1016/s0896-6273\(00\)80509-7](https://doi.org/10.1016/s0896-6273(00)80509-7)
- Madisen, L., Zwingman, T. A., Sunkin, S. M., Oh, S. W., Zariwala, H. A., Gu, H., Ng, L. L., Palmiter, R. D., Hawrylycz, M. J., Jones, A. R., Lein, E. S., & Zeng, H. (2010). A robust and high-throughput Cre reporting and characterization system for the whole mouse brain. *Nature Neuroscience*, 13(1), 133–140. <https://doi.org/10.1038/nn.2467>
- Marsh, D. J., Weingarh, D. T., Novi, D. E., Chen, H. Y., Trumbauer, M. E., Chen, A. S., Guan, X.-M., Jiang, M. M., Feng, Y., Camacho, R. E., Shen, Z., Frazier, E. G., Yu, H., Metzger, J. M., Kuca, S. J., Shearman, L. P., Gopal-Truter, S., MacNeil, D. J., Strack, A. M., ... Qian, S. (2002). Melanin-concentrating hormone 1 receptor-deficient mice are lean, hyperactive, and hyperphagic and have altered metabolism. *Proceedings of the National Academy of Sciences*, 99(5), 3240–3245. <https://doi.org/10.1073/pnas.052706899>

- Mitrofanis, J. (2005). Some certainty for the “zone of uncertainty”? Exploring the function of the zona incerta. *Neuroscience*, *130*(1), 1–15. <https://doi.org/10.1016/j.neuroscience.2004.08.017>
- Monzon, M. E., de Souza, M. M., Izquierdo, L. A., Izquierdo, I., Barros, D. M., & de Barioglio, S. R. (1999). Melanin-concentrating hormone (MCH) modifies memory retention in rats ☆. *Peptides*, *20*(12), 1517–1519. [https://doi.org/10.1016/S0196-9781\(99\)00164-3](https://doi.org/10.1016/S0196-9781(99)00164-3)
- Mouri, T., Takahashi, K., Kawauchi, H., Sone, M., Totsune, K., Murakami, O., Itoi, K., Ohneda, M., Sasano, H., & Sasano, N. (1993). Melanin-concentrating hormone in the human brain. *Peptides*, *14*(3), 643–646. [https://doi.org/10.1016/0196-9781\(93\)90158-d](https://doi.org/10.1016/0196-9781(93)90158-d)
- Nelson, A. B., Krispel, C. M., Sekirnjak, C., & du Lac, S. (2003). Long-lasting increases in intrinsic excitability triggered by inhibition. *Neuron*, *40*(3), 609–620. [https://doi.org/10.1016/s0896-6273\(03\)00641-x](https://doi.org/10.1016/s0896-6273(03)00641-x)
- Noble, E. E., Hahn, J. D., Konanur, V. R., Hsu, T. M., Page, S. J., Cortella, A. M., Liu, C. M., Song, M. Y., Suarez, A. N., Szujewski, C. C., Rider, D., Clarke, J. E., Darvas, M., Appleyard, S. M., & Kanoski, S. E. (2018). Control of Feeding Behavior by Cerebral Ventricular Volume Transmission of Melanin-Concentrating Hormone. *Cell Metabolism*. <https://doi.org/10.1016/j.cmet.2018.05.001>
- Porkka-Heiskanen, T., Strecker, R. E., Thakkar, M., Bjørkum, A. A., Greene, R. W., & McCarley, R. W. (1997). Adenosine: A Mediator of the Sleep-Inducing Effects of Prolonged Wakefulness. *Science*, *276*(5316), 1265–1268. <https://doi.org/10.1126/science.276.5316.1265>
- Presse, F., Sorokovsky, I., Max, J.-P., Nicolaidis, S., & Nahon, J.-L. (1996). Melanin-concentrating hormone is a potent anorectic peptide regulated by food-deprivation and glucopenia in the rat. *Neuroscience*, *71*(3), 735–745. [https://doi.org/10.1016/0306-4522\(95\)00481-5](https://doi.org/10.1016/0306-4522(95)00481-5)
- Qu, D., Ludwig, D. S., Gammeltoft, S., Piper, M., Pellemounter, M. A., Cullen, M. J., Mathes, W. F., Przypek, J., Kanarek, R., & Maratos-Flier, E. (1996). A role for melanin-concentrating hormone in the central regulation of feeding behaviour. *Nature*, *380*(6571), 243–247. <https://doi.org/10.1038/380243a0>
- Rogge, G., Jones, D., Hubert, G. W., Lin, Y., & Kuhar, M. J. (2008). CART peptides: regulators of body weight, reward and other functions. *Nature Reviews Neuroscience*, *9*(10), 747–758. <https://doi.org/10.1038/nrn2493>
- Saito, Y., Cheng, M., Leslie, F. M., & Civelli, O. (2001). Expression of the melanin-concentrating hormone (MCH) receptor mRNA in the rat brain. *The Journal of Comparative Neurology*, *435*(1), 26–40. <https://doi.org/10.1002/cne.1191>
- Saito, Y., Nothacker, H. P., Wang, Z., Lin, S. H., Leslie, F., & Civelli, O. (1999). Molecular characterization of the melanin-concentrating-hormone receptor. *Nature*, *400*(6741), 265–269. <https://doi.org/10.1038/22321>
- Segal-Lieberman, G., Bradley, R. L., Kokkotou, E., Carlson, M., Trombly, D. J., Wang, X., Bates, S., Myers, M. G., Flier, J. S., & Maratos-Flier, E. (2003). Melanin-concentrating

- hormone is a critical mediator of the leptin-deficient phenotype. *Proceedings of the National Academy of Sciences of the United States of America*, 100(17), 10085–10090. <https://doi.org/10.1073/pnas.1633636100>
- Sherin, J. E., Shiromani, P. J., McCarley, R. W., & Saper, C. B. (1996). Activation of ventrolateral preoptic neurons during sleep. *Science (New York, N.Y.)*, 271(5246), 216–219. <https://doi.org/10.1126/science.271.5246.216>
- Shimada, M., Tritos, N. A., Lowell, B. B., Flier, J. S., & Maratos-Flier, E. (1998). Mice lacking melanin-concentrating hormone are hypophagic and lean. *Nature*, 396(6712), 670–679. <https://doi.org/10.1038/25341>
- Sita, L. V., Elias, C. F., & Bittencourt, J. C. (2003). Dopamine and melanin-concentrating hormone neurons are distinct populations in the rat rostromedial zona incerta. *Brain Research*, 970(1–2), 232–237. [https://doi.org/10.1016/S0006-8993\(03\)02345-X](https://doi.org/10.1016/S0006-8993(03)02345-X)
- Skofitsch, G., Jacobowitz, D. M., & Zamir, N. (1985). Immunohistochemical localization of a melanin concentrating hormone-like peptide in the rat brain. *Brain Research Bulletin*. [https://doi.org/10.1016/0361-9230\(85\)90213-8](https://doi.org/10.1016/0361-9230(85)90213-8)
- Smith, D. G., Davis, R. J., Rorick-Kehn, L., Morin, M., Witkin, J. M., McKinzie, D. L., Nomikos, G. G., & Gehlert, D. R. (2006). Melanin-concentrating hormone-1 receptor modulates neuroendocrine, behavioral, and corticolimbic neurochemical stress responses in mice. *Neuropsychopharmacology : Official Publication of the American College of Neuropsychopharmacology*, 31(6), 1135–1145. <https://doi.org/10.1038/sj.npp.1300913>
- Smith, Y., Koylu, E. O., Couceyro, P., & Kuhar, M. J. (1997). Ultrastructural localization of CART (cocaine- and amphetamine-regulated transcript) peptides in the nucleus accumbens of monkeys. *Synapse (New York, N.Y.)*, 27(1), 90–94. [https://doi.org/10.1002/\(SICI\)1098-2396\(199709\)27:1<90::AID-SYN10>3.0.CO;2-V](https://doi.org/10.1002/(SICI)1098-2396(199709)27:1<90::AID-SYN10>3.0.CO;2-V)
- Steriade, M., Gloor, P., Llinás, R. R., Lopes de Silva, F. H., & Mesulam, M. M. (1990). Report of IFCN Committee on Basic Mechanisms. Basic mechanisms of cerebral rhythmic activities. *Electroencephalography and Clinical Neurophysiology*, 76(6), 481–508. [https://doi.org/10.1016/0013-4694\(90\)90001-z](https://doi.org/10.1016/0013-4694(90)90001-z)
- Tortorolo, P., Lagos, P., Sampogna, S., & Chase, M. H. (2008). Melanin-concentrating hormone (MCH) immunoreactivity in non-neuronal cells within the raphe nuclei and subventricular region of the brainstem of the cat. *Brain Research*, 1210, 163–178. <https://doi.org/10.1016/j.brainres.2008.02.104>
- Van Den Pol, A. N., Acuna-Goycolea, C., Clark, K. R., & Ghosh, P. K. (2004). Physiological properties of hypothalamic MCH neurons identified with selective expression of reporter gene after recombinant virus infection. *Neuron*. [https://doi.org/10.1016/S0896-6273\(04\)00251-X](https://doi.org/10.1016/S0896-6273(04)00251-X)
- van den Pol, A. N., Acuna-Goycolea, C., Clark, K. R., & Ghosh, P. K. (2004). Physiological properties of hypothalamic MCH neurons identified with selective expression of reporter gene after recombinant virus infection. *Neuron*, 42(4), 635–652. [https://doi.org/10.1016/s0896-6273\(04\)00251-x](https://doi.org/10.1016/s0896-6273(04)00251-x)

- Varas, M., Pérez, M., Ramírez, O., & de Barioglio, S. R. (2002). Melanin concentrating hormone increase hippocampal synaptic transmission in the rat. *Peptides*, *23*(1), 151–155. [https://doi.org/10.1016/s0196-9781\(01\)00591-5](https://doi.org/10.1016/s0196-9781(01)00591-5)
- Vaughan, J. M., Fischer, W. H., Hoeger, C., Rivier, J., & Vale, W. (1989). Characterization of melanin-concentrating hormone from rat hypothalamus. *Endocrinology*. <https://doi.org/10.1210/endo-125-3-1660>
- Verret, L., Goutagny, R., Fort, P., Cagnon, L., Salvert, D., Léger, L., Boissard, R., Salin, P., Peyron, C., & Luppi, P. H. (2003). A role of melanin-concentrating hormone producing neurons in the central regulation of paradoxical sleep. *BMC Neuroscience*. <https://doi.org/10.1186/1471-2202-4-19>
- Vetrivelan, R., Kong, D., Ferrari, L. L., Arrigoni, E., Madara, J. C., Bandaru, S. S., Lowell, B. B., Lu, J., & Saper, C. B. (2016). Melanin-concentrating hormone neurons specifically promote rapid eye movement sleep in mice. *Neuroscience*. <https://doi.org/10.1016/j.neuroscience.2016.08.046>
- Wang, J., Chen, S., Nolan, M. F., & Siegelbaum, S. A. (2002). Activity-Dependent Regulation of HCN Pacemaker Channels by Cyclic AMP. *Neuron*, *36*(3), 451–461. [https://doi.org/10.1016/S0896-6273\(02\)00968-6](https://doi.org/10.1016/S0896-6273(02)00968-6)
- Wang, X., Chou, X.-L., Zhang, L. I., & Tao, H. W. (2020). Zona Incerta: An Integrative Node for Global Behavioral Modulation. *Trends in Neurosciences*, *43*(2), 82–87. <https://doi.org/10.1016/j.tins.2019.11.007>
- Yin, K., Jin, J., Zhu, X., Yu, L., Wang, S., Qian, L., Han, L., & Xu, Y. (2017). CART modulates beta-amyloid metabolism-associated enzymes and attenuates memory deficits in APP/PS1 mice. *Neurological Research*, *39*(10), 885–894. <https://doi.org/10.1080/01616412.2017.1348689>
- Zamir, N., Skofitsch, G., Bannon, M. J., & Jacobowitz, D. M. (1986). Melanin-concentrating hormone: Unique peptide neuronal system in the rat brain and pituitary gland. *Proceedings of the National Academy of Sciences of the United States of America*. <https://doi.org/10.1073/pnas.83.5.1528>
- Zhang, X., & van den Pol, A. N. (2017). Rapid binge-like eating and body weight gain driven by zona incerta GABA neuron activation. *Science (New York, N.Y.)*, *356*(6340), 853–859. <https://doi.org/10.1126/science.aam7100>



## APPENDIX A: ANIMAL CARE ETHICS APPROVAL

Your Animal Use Protocol has been renewed

**Subject:** Your Animal Use Protocol has been renewed  
**From:** ambakwe@mun.ca  
**Date:** 5/10/2021, 3:45 PM  
**To:** "Hirasawa Michiru(Principal Investigator)" <michiru@mun.ca>  
**CC:** ambakwe@mun.ca



Dear: Dr. Michiru Hirasawa, Faculty of Medicine\Division of BioMedical Sciences

Researcher Portal File No.: 20211649  
 Animal Care File: 18-02-MH  
 Entitled: (18-02-MH) Effect of diet on the hypothalamic function  
 Status: Active  
 Related Awards:

Awards File No	Title	Status	
20171018	Mechanism for high fat diet-induced activation of MCH neurons and its role in obesity	Active	1. Research Grant and Contract Services (RGCS) – St. John's and Grenfell Campuses
20192001	Prostaglandin-E2-mediated activation of melanin-concentrating hormone neurons in diet-induced obesity	Active	1. Research Grant and Contract Services (RGCS) – St. John's and Grenfell Campuses
20192507	Material Transfer Agreement	Active	1. Research Grant and Contract Services (RGCS) – St. John's and Grenfell Campuses

### Ethics Clearance Terminates: May 01, 2024

Your Animal Use Protocol has been renewed for a three-year term. This file replaces the previous File ID [[20181358]]; while the Animal Care ID [[18-02-MH]] remains the same as the active ethics clearance associated with this project. Please note the new file ID (if required) when referring to this protocol.

This ethics clearance includes the following Team Members: Dr. Michiru Hirasawa (Principal Investigator)

This ethics clearance includes the following related awards:

Awards File No	Title	Status	

Your Animal Use Protocol has been renewed

20171018	Mechanism for high fat diet-induced activation of MCH neurons and its role in obesity	Active	1. Research Grant and Contract Services (RGCS) – St. John's and Grenfell Campuses
20192001	Prostaglandin-E2-mediated activation of melanin-concentrating hormone neurons in diet-induced obesity	Active	1. Research Grant and Contract Services (RGCS) – St. John's and Grenfell Campuses
20192507	Material Transfer Agreement	Active	1. Research Grant and Contract Services (RGCS) – St. John's and Grenfell Campuses

An Event [Annual Report] will be required following each year of protocol activity.

Should you encounter an unexpected incident that negatively affects animal welfare or the research project relating to animal use, please submit an Event [Incident Report].

Any alterations to the protocol requires prior submission and approval of an Event [Amendment].

**NOTE:** You can access a copy of this email at any time under the "Shared Communications" section of the Logs tab of your file in the [Memorial Researcher Portal](#).

Sincerely,

**ANULIKA MBAKWE | ACC COORDINATOR**

Department of Animal Care Services  
Memorial University of Newfoundland  
Health Sciences Centre | Room H1848  
P: 709-777-6621  
E-Mail: [ambakwe@mun.ca](mailto:ambakwe@mun.ca)